Volume 3 Issue 1 · April 2019

ISSN 2591-7110 (print) ISSN 2591-7129 (online)

April

2019

MODERN ELECTRONIC TECHNOLOGY

01

SYNERGY PUBLISHING PTE. LTD.

SYNERGY PUBLISHING PTE. LTD.

Modern Electronic Technology

Aims and Scope

Modern Electronic Technology (MET) is an open access, peer-reviewed scholarly journal which aims to publish original research articles, reviews and short communications that covers all area of electronic engineering technology. MET emphasizes on publishing high quality papers, as well as aims to provide a source of information and discussion platform for engineers, researchers, and electronic professionals worldwide.

Subject areas suitable for publication include, but are not limited to the following fields:

- Microelectronics
- Nanoelectronics
- Electronic Materials Technology
- Structure and Nature of Semiconductor
- Digital Technology
- Automation System

Publishing Cycle

Quarterly

Journal Homepage

http://ojs.s-p.sg/index.php/met

Key Features

- Open Access
- High Academic Level Editorial Board
- Easy and Fast Submissions
- Double Blind Peer Review
- Rapid Online Publication of Articles upon Acceptance
- Outlet for Academic Institutions and Industry

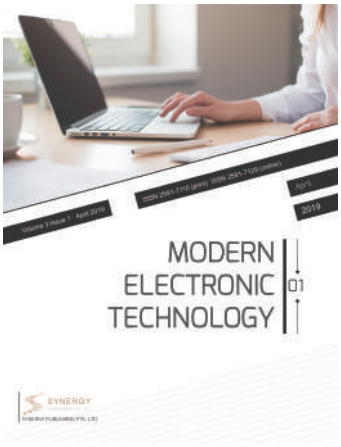

Volume 3 Issue 1 • April 2019
ISSN 2591-7110 (print) ISSN 2591-7129 (online)

Synergy Publishing Pte. Ltd.

E-Mail: contact@s-p.sg
Official Website: www.s-p.sg
Address: 12 Eu Tong Sen Street,
#08-169, Singapore (059819)

CONTENTS

Article

Review

SYNERGY PUBLISHING PTE. LTD.

Modern Electronic Technology

https://ojs.s-p.sg/index.php/met

ARTICLE

Analysis of the Influence of Different Plastic Packaging Materials on Product Delamination of IC Components

Dongmei Liu*, Wenhe Wang, Zhenjiang Pang, Lianhe Ji, Jian Wang, Zhengqiang Yu, Pingping Zheng

Department of Quality Control, Beijing Smart-Chip Microelectronics Technology Co., Ltd., Beijing, 100192, China

ARTICLE INFO

Article history
Received: 12 October 2018
Revised: 25 March 2019
Accepted: 8 April 2019
Published Online: 16 April 2019

Keywords:
Plastic package
Hygroscopicity
Cohesiveness
Stress
Delamination
Improvement

ABSTRACT

Due to the high hygroscopicity of the plastic packaging material, the device is inevitably subjected to high temperature or high humidity environment during the production and testing process. After the moisture is expanded, the internal stress is too large, and the delamination and gold wire breakage are formed. At the same time, due to the difference in the coefficient of thermal expansion (CTE) between the plastic packaging material and the materials such as Si and Cu, it is easy to form delamination under a relatively large shear force. The water vapor remaining in the plastic packaging material is the root cause of delamination, and the reflow process and temperature are the predisposing factors leading to delamination. However, it has been found through experiments that different plastic packaging materials have different hygroscopicity and cohesiveness, and they have obvious improvement effects on delamination.

1. Epoxy Resin Plastic Package for IC Components

The package is a must for the chip and is also critical. The package not only protects the chip, but also enhances its thermal conductivity. It is a bridge between the internal and external circuits of the chip.

The plastic package is a package form of a component shell using a polymer-synthesized epoxy resin. The IC package not only requires excellent electrical conductivity, thermal conductivity, and mechanical properties of the packaging material, but also requires high reliability and environmental friendliness of the plastic package. The plastic sealing function is to provide physical protection to the chip, prevent impurities in the air from corroding the chip circuit, cause electrical performance degradation, and protect the chip surface and connecting leads from external damage and external environment. The thermal expansion coefficient of the chip is matched with the thermal expansion coefficient of the frame or the substrate by the package, thereby alleviating the stress generated by the

**Corresponding Author:*
Dongmei Liu,
Department of Quality Control, Beijing Smart-Chip Microelectronics Technology Co., Ltd., No. 66 Xixiaokou Road, Dongsheng Science and Technology Park, Zhongguancun, Haidian District, Beijing, 100192, China;
E-mail: 71102478@qq.com.

 DOI: https://doi.org/10.26549/met.v3i1.1527

change of the external environment such as heat and the stress generated by the heat generated by the chip, thereby preventing chip damage and failure.

The advantages of plastic package: light weight, small size, low cost and simple manufacturing process. At the same time, plastic packaging is widely used in IC component packaging and processing operations, which greatly improves the production efficiency of electronic components.

The disadvantages of plastic package: The plastic sealing material is easy to absorb moisture, and the moisture in the air easily penetrates into the device through the plastic sealing material. The plastic packaging material is a polymer synthetic material, and the inside thereof inevitably contains various impurities (Cl^-, Na^+ plasma, etc.). The presence of impurity ions and water vapor will also have an effect on the internal delamination of the component. In severe cases, the "popcorn" effect occurs during subsequent SMT reflow processing.

2. The Composition of Epoxy Resin

The epoxy resin contains an epoxy group in its molecular structure and is a multi-component polymer composite, under the action of heat and curing agent, the epoxy group chemically reacts with the curing agent phenolic resin to produce cross-linking curing, which becomes a thermosetting plastic, after curing, the epoxy resin has good physical and chemical properties. It has excellent bonding strength to the surface of metal and non-metal materials, good dielectric properties, small set shrinkage, good stability, high hardness and good flexibility. The epoxy resin includes various organic and inorganic components, such as: o-cresol novolac epoxy resin, novolac resin, filler silica powder (commonly known as silicon micropowder), accelerator, coupling agent, modifier, flame retardant, colorant and other components.

Its basic composition and roles are as follows:

Table 1. The basic composition and roles of epoxy resin

Composition	Composition / %	Main Roles
Polymers	Epoxy resin: 5~20	Basic resin, polymerization, bonding
	Curing agent: 3~10	Cross-linking reaction
Catalysts	Coupling agent: <1	Bridge of inorganic and organic matter
Fillers	Curing accelerator: <1	Speed up the cross-linking reaction
	Packing: 70~92	Improve physical properties, reduce expansion coefficient, water absorption and cost
Additives	Release agent: <2	Improve mold release performance and improve fluidity
	Flame retardant: <3	Meet UL-94 requirements
	Colorant: <0.5	colors
	Ion adjuvant: <1	Improve reliability
	Stress absorber: <2	Reduce internal stress
	Binder: <0.5	Improve L/F, ST adhesion

3. Effect of Hygroscopicity on IC Components

3.1 Delamination and Corrosion Failure

Since the epoxy resin package is a non-hermetic package, the tolerance and ability to the external environment are poor. When the epoxy resin is exposed to a humid environment, it has strong water vapor hygroscopicity. [1] On the one hand, in a humid environment, water vapor diffuses inward along the interface of the molding body and the molding body and the pin, and enters the surface of the device chip; on the other hand, due to the certain water absorption of the resin itself, water vapor is directly diffused to the surface of the chip through the molding material. The inhaled moisture, if it has more ion contaminants, will cause corrosion of the bonding area of the chip. If there is a defect in the passivation layer on the surface of the chip, moisture will invade the metallization layer of the chip.[2] Regardless of the corrosion of the bonding area or the corrosion of the metallization layer, the mechanism can be attributed to the chemical reaction of the metal lead and the ionized dirt: Due to the immersion of water vapor, the dissociation of the hydrolyzed substance (Cl^-, Na^+ plasma) from the resin is accelerated, and the substance dissociated during the corrosion process changes due to physical properties, such as an increase in brittleness, an increase in contact resistance value, and a change in thermal expansion coefficient.

During the use or storage of the device, as the temperature and the load voltage change, it will exhibit electrical parameter drift, excessive leakage current, and even short circuit or open circuit failure, which will bury hidden dangers for the long-term reliability of the device,[2-3] the most common phenomenon is the occurrence of stratification. When the package changes in ambient temperature, the sum of the internal stress and the vapor pressure of the moisture is greater than the adhesion between the epoxy resin and the chip, the carrier and the surface of the frame. As a result, peeling occurs between their interfaces, and delamination occurs. In reflow soldering, water vapor expands due to thermal stress caused by rapid heating,

DOI: https://doi.org/10.26549/met.v3i1.1527

which in turn causes device failure.

3.2 "Popcorn" Failure

There are three sources of heat that the molded electronics conduct to the device during soldering: infrared reflow heating, vapor reflow heating, and wave soldering heating. The infrared reflow soldering temperature is 235~240°C, the time is about 10S; the vapor reflow soldering temperature is 215±5°C, the time is about 40s; the wave soldering heating temperature is 260±5°C, and the time is about 5S. During the heating process of the plastic electronic device, the moisture adsorbed in the plastic body is rapidly vaporized, and the internal water vapor pressure is too large, so that the epoxy resin expands, and delamination and cracking occur, which is commonly called "popcorn" failure. However, in the case that the plastic body does not fail during welding, but the plastic body is cracked due to moisture and thermal expansion or cooling or shrinkage, the crack will corrode the dirt and moisture into the passage, which affects long-term reliability in later use. At the same time, in the welding, the epoxy resin will expand due to heat, and the shear stress generated inside the epoxy resin will affect the integrity of the bonding wire. The corner stress of the chip is relatively concentrated, which may cause the bonding wire to be lifted, the bonding point to be cracked, or the bonding wire to be broken, resulting in failure of electrical performance.

4. The Delamination of IC Components

In component packaging, delamination is a major aspect of reliability evaluation. The delamination is a slight peeling or cracking between the interfaces inside the molded body (PKG).

Most delamination occurs at the interface of the internal material of the package, including between the encapsulating resin and the chip interface, between the encapsulating resin and the substrate interface, between the chip and the bonding material interface, between the bonding material and the substrate interface, and inside the bonding material, etc. The delamination phenomenon occurs at the interface between the plastic resin of the plastic package device and other materials, which may cause device performance degradation or even failure. For example, if the delamination occurs at the interface between the resin and the chip, it will not only cause the bond wire of the chip to be mechanically damaged due to mechanical stretching or bond wire, but the connection resistance is increased or opened; it may also cause damage to the passivation layer on the surface of the chip, resulting in increased chip leakage, etc.; or delamination of the interface between the resin and the chip, which makes it easier for water vapor to enter the surface of the chip, degrading the performance of the chip. The interface between the epoxy resin and other materials in the molding device is delamination. Even if the delamination area is small, the adhesion of the delamination part is seriously reduced, and the structural stress is also changed. In the subsequent device use, due to the effect of thermal strain or mechanical stress, the delamination condition is intensified, and as the delamination area increases, the device eventually fails.

There are many factors leading to delamination, in which the plastic sealing resin, chip, frame and the like are different due to different materials, the thermal expansion coefficient is different at high temperature, and the CTE mismatch between the plastic sealing material, the chip and the frame causes shearing force on the contact surface.

When the components are in the SMT process, when the device is in a high temperature state, the reflow soldering environment temperature rises rapidly to about 260 °C, the stress inside the laminator is concentrated due to thermal expansion for a short time. In addition, the moisture accumulated in the encapsulation interface layer diffuses into the micro-cavities, and the wet heat stress and the rapidly rising pressure in a short time may cause the package to fail.[4] The diffusion of moisture and the formation of high pressure conditions also led to the occurrence of delamination. The process of delamination and even cracking caused by the plastic components after moisture absorption under high temperature conditions can be simply expressed as follows:

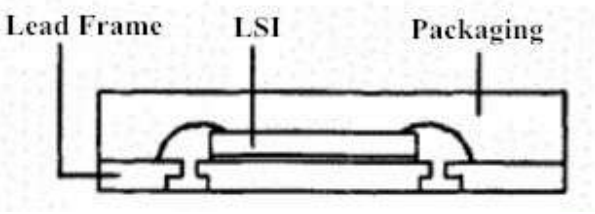

Figure 1. Plastic components before hygroscopicity

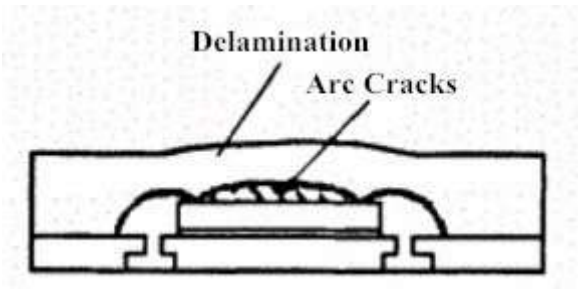

Figure 2. Vapor expansion and delamination under high temperature conditions

 DOI: https://doi.org/10.26549/met.v3i1.1527

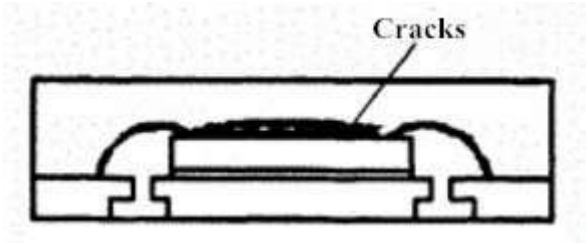

Figure 3. Occurrence mechanism of Packaging delamination and cracks

5. Effect of Different Plastic Packaging Materials on Packaging, Hygroscopicity and Delamination

The characteristics of epoxy resin are the basic factors leading to delamination inside the plastic body.[5] In the package, the adhesion of the epoxy resin to the frame, coefficient of thermal expansion (CTE), the strength and the conductivity of the material have a significant effect on the internal delamination of the plastic body. The differences in elongation, hygroscopicity and adhesion of epoxy resin also have different effects on delamination.[6]

In materials selecting, the first thing to consider is the adhesion between the epoxy resin and the frame. In addition to the necessary physical bonding, it is more important that a certain chemical bond can occur between the epoxy resin and the frame to ensure better bonding performance. The occurrence of chemical bonding will have a more powerful influence on the structural strength of the plastic-sealed components, resulting in a tighter bond between the epoxy resin and the chip, the carrier, and the frame, thereby improving the mechanical structure and reliability of the device. Electronic components with good and reasonable mechanical structure can maintain excellent reliability even under reflow soldering. In order to evaluate the influence of different molding materials on the package, two epoxy resins were specially selected for package verification and comparative analysis.

The composition and characteristics of the two materials are compared as follows:

Table 2. Comparison of the composition and characteristics of two epoxy resins

Type	Compound 1	Compound 2
Series	700	8240
Remark	Contain adhesion promoters	NA
Filler content	87	88.5
Filler type	Spherical	Spherical
Filler sieved size(um)	75	75
Epoxy type	MAR	LMWE9+MA
Hardener	MAR	LWAH2
Flame retardant	MAR	NA
Spiral flow(cm)	135	101
Gel time	50	35
CTE1(PPM)	10	9
CTE2(PPM)	39	32
Tg	125	120
Flexural strength RT (kgf/mm2)	17	15
Flexural modulus RT (kgf/mm2)	2250	2500
Water absorption (%)	0.13	0.3

By comparing the composition and characteristics of the two epoxy materials, it is found that the thermal expansion coefficients of the two resins are relatively close, and there is no significant difference in the coefficient of thermal expansion between the two. However, the 700 resin is compared with the 8240 resin, the former contains a binding accelerator, and the water content is also lower. The wafers were selected from different batches of different batches, and the two resins were used for package verification. After on-line verification and reliability evaluation, it was found that: the components encapsulated with 700 resin have better bonding strength between epoxy resin and other materials, and can better improve the phenomenon of delamination of 8240 resin.

Table 3. Effect of two epoxy resins on delamination

Leg	Compound	SAT 0 Delam Qty	TCT 200 cycles Delam Qty	TCT 500 cycles Delam Qty	TCT 800 cycles Delam Qty
1	700	0/77ea	0/77ea	0/77ea	0/77ea
2	8240	0/77ea	1/77ea	2/77ea	4/77ea

Through reliability test verification and evaluation, it was found that the resin of 700 exhibited better performance than the 8240 resin in the experiments of TCT200, TCT500 and TCT800, and the structural adhesion, product moisture absorption and delamination improvement of the product package were greatly improved. And through the subsequent multi-batch, large-volume package verification and regular sample tracking and evaluation results, the stability and reliability of 700 resin is better than 8240 resin with high hygroscopicity and no adhesion promoter.

6. Conclusion

In the interior of the plastic body, there is a problem of interfacial adhesion between the epoxy resin and the surface of the chip, the lead frame, and the carrier. The use of an epoxy resin with a bonding accelerator can better improve and enhance the problem of interface adhesion, improve the bonding firmness of the interface, and at the same time effectively enhance the packaging structure and strength of the molding body.

DOI: https://doi.org/10.26549/met.v3i1.1527

Through analysis and research, it was found that the internal delamination of the plastic body can be achieved by using a less hygroscopic epoxy resin, and by selecting an epoxy resin containing a binding force promoter, increasing the adhesion between the resin and the frame, the chip, the carrier, and enhancing the structural strength, an effective improvement is obtained. In addition, there are many reasons for the occurrence of delamination inside the plastic package. In addition to the analysis and research by changing the angle of epoxy resin, we can also try to explore the optimization of package structure design, frame design, and packaging process improvement, increasing the structural strength, bonding force and reducing the risk of moisture absorption inside the plastic body can more effectively reduce or avoid the occurrence of delamination inside the plastic body.

References

[1] CHEN X, ZHAO S. Moisture absorption and diffusion characterization of molding compound[J]. Journal of Electronic Packaging, 2005, 127:460-465.

[2] Linchun Zhang. Evaluation of moisture absorption sensitivity level of green plastic IC[J]. Electronics Process Technology, 2005, 26(6):336-338. (in Chinese)

[3] Lanxia Li. The problem of hygroscopic cracking of surface mount plastic enclosure and its countermeasures[J]. Electronics and Packaging, 2005, 5(10):14-18. (in Chinese)

[4] Jun Wang, Fan Yang, Zhen Lu. Analysis of delamination fracture of electronic components package caused by damp heat[J]. Journal of Southwest Jiaotong University, 2002, 37(2):125-128. (in Chinese)

[5] Xin Li, Yi Zhou, Chengsong Sun. Research progress on failure mechanism of plastic encapsulated microelectronic devices[J]. Semiconductor Technology, 2008, 33(2):98-101. (in Chinese)

[6] Guangchao Xie. Relationship between encapsulating resin and PKGdelamination[J]. Electronics and Packaging, 2006, 6(2):20-23. (in Chinese)

 DOI: https://doi.org/10.26549/met.v3i1.1527

SYNERGY PUBLISHING PTE. LTD.

Modern Electronic Technology

https://ojs.s-p.sg/index.php/met

ARTICLE

Promote the Compression Efficiency of Digital Images by Using Improved CUR Matrix Decomposition Algorithm

Qinghai Jin*

Yunnan Minzu University, Kunming, Yunnan, 650504, China

ARTICLE INFO

Article history
Received: 2 November 2018
Revised: 26 March 2019
Accepted: 8 April 2019
Published Online: 16 April 2019

Keywords:
Image compression
Standard deviation sampling
CUR matrix decomposition
Singular value decomposition
SVD-CUR

ABSTRACT

In order to overcome the problem that the CUR matrix decomposition algorithm loses a large amount of information when compressing images, the quality of reconstructed images is not high, we propose a CUR matrix decomposition algorithm based on standard deviation sampling. Because of retaining more image information, the reconstructed image quality is higher under the same compression ratio. At the same time, in order to further reduce the amount of image information lost during the sampling process of the CUR matrix decomposition algorithm, we propose the SVD-CUR algorithm. The experimental results verify that our algorithm can achieve high image compression efficiency, and also demonstrate the high precision and robustness of CUR matrix decomposition algorithm in dealing with low rank sparse matrix data.

1. Introduction

With the advent of the digital age, large amounts of image information can put tremendous pressure on the storage capacity of the memory, the bandwidth of the communication trunk channel, and the processing speed of the calculation. To solve these problems, we need to compress the image data during its transmission and storage. Commonly used image compression coding methods can be divided into lossy coding and lossless coding. Since lossy compression generally achieves a higher compression ratio, it is an ideal coding option when the quality of the image is not very high.

We often represent the grayscale image as a two-dimensional array (matrix), and RGB images are represented by an M×N×3 multidimensional data matrix. Thus, our processing of digital images can be, in a sense, an operation on the digital matrix of images. In recent years, with the continuous development and improvement of applied mathematics, the application of matrix algebra in various subject areas has become more and more extensive. In 2006, a digital image compression coding method based on matrix singular value decomposition (SVD)[1,2] theory appeared.[3] The basic idea is to transform the original image matrix into a low-rank approximation matrix by the singular value decomposition technique of the matrix, reduce the amount of data needed to represent the image, and reduce the resources occupied by the image. In addition, SVD plays an important role in large-scale matrix dimensionality reduction, such as in complex networks,[4]

**Corresponding Author:*
Qinghai Jin,
Yunnan Minzu University, No. 2929 Yuehua Street, Chenggong District, Kunming, Yunnan, 650504, China;
E-mail: jinqinghai2016@163.com.

DOI: https://doi.org/10.26549/met.v3i1.1185

feature discovery.[5-7]

The CUR decomposition of the matrix[8-10] can avoid the low-rank approximation of the original matrix by avoiding the eigenvalue solution for the high-dimensional matrix.[11-14] We consider applying it to image data compression. For the characteristics of image data, we propose a CUR matrix decomposition algorithm based on standard deviation sampling. Furthermore, we combine CUR and SVD, two matrix decomposition-based data reduction algorithms, which effectively overcome the shortcomings of the CUR decomposition algorithm and can greatly reduce the scale of the image.

2. Matrix CUR Decomposition Algorithm and Its Improvement

2.1 Matrix CUR Decomposition

2.1.1 Definition 1

Let A be a matrix of m×n, and C be an m×c (general c < n) submatrix of A, R is an r×n (general r < m) submatrix of A, U is a c×r matrix, then matrix $\widetilde{A}$ is a low rank approximation (CUR approximation) based on row and column selection of A, i.e.

$$A \approx \widetilde{A}=CUR \tag{1}$$

Where U is a normal matrix, U=C+AR+, and C+ and R+ are respectively the Moore-Penrose inverses of C and R. The CUR decomposition structure of the matrix can be simply expressed as follows:

Figure 1. The schematic diagram of matrix CUR decomposition

2.1.2 Definition 2

If there are linear equations (in Moore-Penrose inverses): $Ax=b$, $A \in C^{m\times n}$, $b \in Cm$, and $X \in C^{m\times n}$, and if there is an arbitrary b, the linear equations have solutions: $x=Xb$, $X=A^{+}b$, then matrix $A^{+} \in C^{m\times n}$ is called the Moore-Penrose inverse of A. Obviously, the above definition must also be true for the real matrix.

2.2 Algorithm 1: CUR Matrix Decomposition Algorithm

Input: the original image matrix $A \in R^{m\times n}$

Output: the approximate matrix $\widetilde{A} \in R^{m\times n}$

(1) Randomly extract c ($c \le n$) columns from A to form submatrix $C \in Rm\times c$;

(2) Randomly extract r ($r \le m$) rows from A to form submatrix $R \in Rr\times n$;

(3) Calculate the normal matrix $U=C^{+}AR^{+}$, in which C^{+} and R^{+} are respectively the Moore-Penrose inverses of C and R;

(4) Return to the approximate matrix $\widetilde{A}=CUR$ of the original matrix A.

2.3 Improved CUR Matrix Decomposition Algorithm

The CUR matrix decomposition algorithm has strong randomness and instability in the process of constructing submatrices C and R, which makes the constructed matrices U and $\widetilde{A}$ uncertain, the error is large, and the randomly extracted columns or rows, due to their atypicality, will cause the loss of many important information of the original image matrix.

We select an RGB image of jpg[15-16] format of 512×512×3 from the international standard test image set and convert it into a double-precision gray image, as shown in Figure 2. Then we use this image as the original image of the subsequent simulation experiment (in the MATLAB environment).

Figure 2. The 512 × 512 original Lena image

We calculate the characteristics of the original image matrix row and column standard deviation distribution as follows.

 DOI: https://doi.org/10.26549/met.v3i1.1185

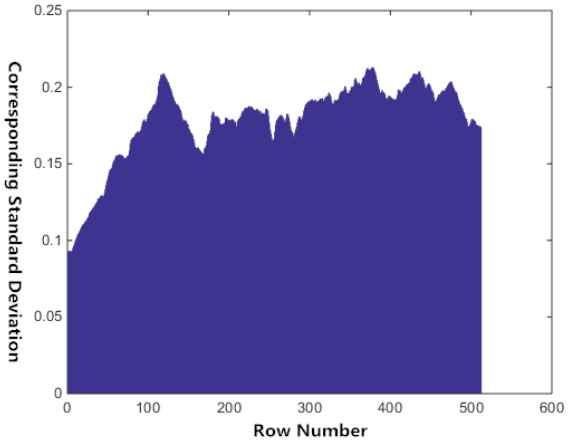

(a) The row standard deviation

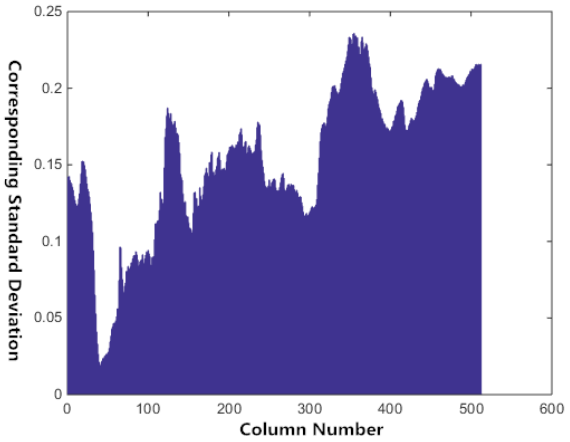

(b) The column standard deviation

Figure 3. Image matrix row and column standard deviation distribution bar graph

As shown in Figure 3, the distribution of the standard deviation of the row and column of the image matrix is very uneven, and the information of the image contained in the row or column with a large standard deviation is large, and the contribution to the image feature is also large. In the CUR decomposition, we construct the sub-matrices R and C by extracting the rows and columns with the largest standard deviation to preserve as much original image information as possible, so that the compressed image quality is higher. The specific algorithm steps are as follows:

Algorithm 2: CUR Decomposition Algorithm Based on Standard Deviation Sampling

Input: the original image matrix $A \in R^{m\times n}$

Output: the approximate matrix $\widetilde{A} \in R^{m\times n}$

(1) Calculate the row and column standard deviation of the original matrix *A*;

(2) Sort the row and column standard deviations in step (1) in order from largest to smallest;

(3) Select the columns and rows corresponding to the first c and the first r maximum standard deviations respectively, and construct the submatrices *C* and *R*;

(4) Construct *U* according to step (3) of Algorithm 1;

(5) Return to the approximate matrix *A* according to step (4) of Algorithm 1.

3. CUR Algorithm Combining SVD

3.1 The Basic Principle of Matrix Singular Value Decomposition (SVD)

Principle 1: Let $A \in Rm\times n$, there are orthogonal matrices $U=[u1, u2, ...,um] \in Rm\times m$, $V=[v1, v2, ...,vn] \in Rn\times n$, and $\{u^t\}_{t=1}^m \in R^m, \{v^t\}_{t=1}^n \in R^n$, which make that,

$$A = U\Sigma V^T \tag{2}$$

Where

$\Sigma = diag(\sigma_1,\cdots,\sigma_\rho) \in R^{m\times n}, \rho = \min\{m,n\}, \sigma_1 \geq \sigma_2 \geq \cdots \geq \sigma_\rho \geq 0, \sigma_i$ is called the singular value of *A*, and vectors ui and vi are called the i-th left and right singular vectors, respectively.

If $k \leq r = rank(A)$, we define $A_k = U_k\Sigma_k V_k^T = \Sigma_{t=1}^k \sigma_t u^t v^{tT}$.

The singular values of any image matrix satisfy the "large L curve" as shown in Figure 4. Larger singular values only account for a small fraction of all singular values. We choose these larger *k* ($k < r$) singular values to approximate the original matrix A, i.e. $Ak \approx A$, which achieves the effect of reducing the rank.

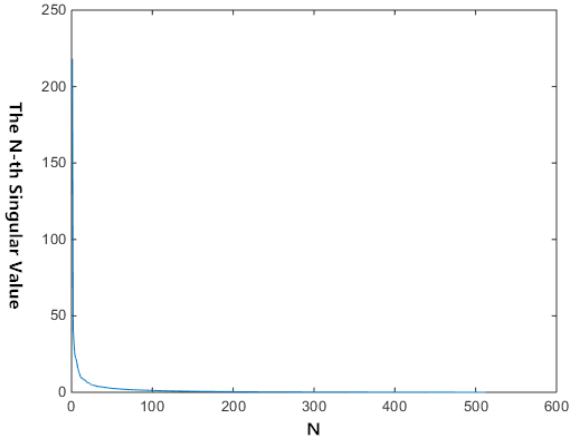

Figure 4. Singular value characteristic curve of the original image

3.2 SVD-CUR Algorithm

Since the image matrix is generally a full rank matrix, direct sampling will lead to a large lack of image informa-

DOI: https://doi.org/10.26549/met.v3i1.1185

tion. We first perform SVD decomposition on the original image matrix, and the reduced rank, reduced rank approximation retains most of the original image. Then, the CUR decomposition of the standard deviation sampling is performed on the low rank matrix, which further reduces the image size, so that the information loss of the reconstructed image is less, and the quality of the reconstructed image is improved. The specific algorithm steps are as follows:

Algorithm 3: SVD-CUR Algorithm

Input: the original image matrix $A \in Rm \times n$

Output: the approximate matrix $\widetilde{A} \in Rm \times n$

(1) Perform SVD decomposition on A;

(2) Select the first k larger singular values and the corresponding singular vectors to construct a low rank matrix Ak;

(3) Gradually further process Ak according to Algorithm 2;

(4) Return to the approximate matrix $\widetilde{A} \in Rm \times n$.

4. Accuracy and Compression Ratio Analysis Based on CUR Decomposition Method

4.1 Accuracy

The error produced by the original matrix after CUR decomposition can be measured by the root mean square distortion ratio (PRD):

$$PRD(\%) = \frac{\|A - CUR\|_F}{\|A\|_F} \tag{3}$$

Where $\|A\|_F = \left(\sum_i \sum_j |a_{ij}|^2 \right)^{\frac{1}{2}}$ is called the Frobenius norm of the matrix.

The root-mean-square distortion ratio is a widely used test method for comparing the reconstruction performance of low-dimensional models. In some specific cases, the error rate is almost zero.

4.2 Compression Ratio

We calculate the ratio of the total number of elements in the original (uncompressed) matrix to the total number of elements in the corresponding low rank approximation matrix by calculating the Compression Ratio (CR).

4.2.1 Compression Ratio of CUR Decomposition

In the matrix CUR decomposition, we approximate the original matrix A by $C \in Rm \times r$, $U \in RC \times r$ and $R \in R-r \times n$, at which point the compression ratio is:

$$Cr_1 = \frac{mn}{mc + cr + rn} \tag{4}$$

Where c and r respectively represent the number of columns and rows stored in the low rank approximation image matrix. The compression ratio formula for CUR decomposition can be improved by the following method:

In the CUR decomposition, we store the original columns and subsets of the data matrix A with C and R, respectively. Obviously, C and R have cr elements that are identical. To improve compression efficiency, we replace the cr redundant data by storing $c+r$ positions of these columns and rows. Therefore, the compression ratio based on CUR decomposition can be optimized to:

$$Cr_2 = \frac{mn}{mc + cr + (rn - cr) + (c + r)} \tag{5}$$

Later, we will use Formula (5) to calculate the compression ratio of the CUR decomposition. It is easy to obtain from this formula, and the larger the $c+r$ is, the larger the number of rows and columns extracted from the original image matrix, the smaller the compression ratio, and the smaller the amount of data compressed by the image. Conversely, the fewer the number of rows and columns extracted, the larger the compression ratio, and the more data the image compresses.

4.2.2 Compression Ratio of SVD-CUR Algorithm

At first, we define the compression ratio of the preprocessed image after SVD decomposition:

$$Cr_3 = \frac{mn}{(m + n + 1)k} \tag{6}$$

Where m and n respectively represent the row and column number of the image data before compression and k represents the number of larger singular values selected.

The compression ratio Cr of the SVD-CUR algorithm is defined as the sum of the compression ratio of the matrix SVD decomposition and the compression ratio of the CUR decomposition, i.e.

$$Cr = Cr_2 + Cr_3 \tag{7}$$

 DOI: https://doi.org/10.26549/met.v3i1.1185

5. Experimental Results and Analysis

5.1 Improved CUR Algorithm Experiment

(a)

(b)

(c)

(d)

(e)

(f)

Figure 5. CUR and its improved algorithm image compression effects

As shown in Figure 5, (a), (b), and (c) are images reconstructed from the digital matrix of Figure 2 by extracting 250, 200, 150 rows and columns according to the sampling method in Algorithm 2; Figures (d), (e), and (f) are images

DOI: https://doi.org/10.26549/met.v3i1.1185

reconstructed after randomly extracting the same number of rows and columns according to Algorithm 1. Obviously, the quality of the reconstructed image of Algorithm 2 is better than Algorithm 1, and the sharpness of the image is gradually decreasing as the number of samples is reduced.

5.2 Experiment of SVD-CUR Algorithm

The simulation experiment of 5.1 shows that the improved CUR algorithm can achieve certain image compression effects when the number of rows and columns is large, but it is not ideal. In the experiment of SVD-CUR algorithm below, after SVD decomposition preprocessing is performed on the image matrix of Figure 2, we carry out the experiment of CUR algorithm by extracting the smaller number of rows and columns, in order to further improve the compression ratio of the image. At the same time, in order to test the sensitivity of the CUR algorithm to the matrix rank before sampling, we divided the experiments into two groups. The ranks of the image matrices before the CUR algorithm were different in the two groups. The simulation results are as follows:

(a)

(b)

(c)

(d)

(e)
Group 1 (when k=64)

 DOI: https://doi.org/10.26549/met.v3i1.1185

(f)

(g)

(h)

(i)

(j)

Group 2 (when k=44)

Figure 6. SVD-CUR algorithm image compression effects

Table 1. Partial statistical characteristics of reconstructed images (Group 1)

Statistical indicators	SVD Decomposition Initialization Image	Sampling Number of Rows and Columns			
		100	80	60	40
Entropy	7.4274	7.4274	7.4274	7.4802	7.4373
Gray average	0.4154	0.4154	0.4154	0.4146	0.4017
Gray Standard Deviation	0.1839	0.1823	0.1823	0.1784	0.1689
Compression Ratio	3.9961	6.1519	6.6908	7.5891	9.3856

Table 2. Partial statistical characteristics of reconstructed images (Group 2)

Statistical indicators	SVD Decomposition Initialization Image	Sampling Number of Rows and Columns			
		100	80	60	40
Entropy	7.4396	7.4396	7.4396	7.4396	7.4857
Gray Average	0.4154	0.4154	0.4154	0.4154	0.4123

DOI: https://doi.org/10.26549/met.v3i1.1185

Gray Standard Deviation	0.1839	0.1811	0.1811	0.1811	0.1768
Compression Ratio	5.8125	7.9683	8.5072	9.4055	11.2020

As shown in FIG. 6, the first group of images is (a)-(e), and the figure (a) is an image reconstructed according to the SVD decomposition principle of the matrix, taking =64 (i.e., singular value less than 2 is ignored). Figures (b)-(e) are images reconstructed sequentially by extracting 100, 80, 60, 40 rows and columns from the original image matrix (a) according to Algorithm 3; the second group of images is (f)-(i), Figure (f) is an image reconstructed with =44 (i.e., singular values less than 3 are ignored). Figures (g)-(j) are images reconstructed according to Algorithm 3 using the same number of samples in Group 1 respectively.

The quality of (a) in the first group is slightly higher than that in the second group (f), which is because when we perform SVD decomposition on the digital matrix of Figure 2, the number of singular values is more selected when reconstructing the image, and more information of the original image is retained.

Although the number of samples in these two groups is relatively small, the quality of image restoration is ideal. The first three images (a), (b), and (c) of the first group are almost indistinguishable, and the first four images (f), (g), (h), and (i) of the second group are almost indistinguishable. Compression is almost "lossless". In contrast, the image restoration quality of the first group decreases more rapidly with the decrease of the number of sample rows and columns, and the image quality of the second group decreases relatively well with the decrease of the number of sample rows and columns which shows that the CUR algorithm has better robustness to low rank matrices.

As shown in Tables 1 and 2, the image quality evaluation results obtained by the naked eye observation image are basically consistent with the partial objective metrics of the reconstructed image, and as the rank of the sampled image matrix decreases and the number of samples decreases, and then we can get a better compression ratio.

6. Conclusion

In order to preserve the image information reconstructed by the traditional CUR matrix decomposition algorithm, we propose a CUR matrix decomposition algorithm based on standard deviation sampling. The most basic evaluation criteria for analyzing the accuracy and compression ratio of CUR matrix decomposition algorithm are also given. Furthermore, we combine the matrix singular value decomposition algorithm and the CUR matrix decomposition algorithm to preprocess the original image matrix by singular value decomposition, and then use the improved CUR matrix decomposition algorithm. The experimental results show that the reconstructed image quality of CUR matrix decomposition algorithm based on standard deviation sampling is higher than the traditional CUR matrix decomposition algorithm, and the approximate image reconstructed by SVD-CUR algorithm can obtain a larger compression ratio, and the image compression effect is ideal and it is still very stable, and it also shows that the CUR algorithm is more suitable for the decomposition processing of low rank sparse matrices.

Next, we consider compressing the face image using the algorithm proposed in this paper, and using the compressed image as the pre-processed image, then performing image segmentation and feature extraction on them, and using pattern recognition technology to classify the face image of the batch. On the other hand, we will also explore the use of this algorithm for image data in specific areas, such as remote sensing images and medical images.

References

[1] Tingzhu Huang, Shouming Zhong, Zhengliang Li. Matrix Theory[M]. Beijing: Higher Education Press, 2003: 94-95. (in Chinese)

[2] Huiping Yuan. Subunitary Matrix and Submirror Array[J]. Journal of Northeast Normal University (Natural Science), 2001, 33(1): 26-29. (in Chinese)

[3] Xiangfeng Hu, Jinmao Wei. Image Compression Based on Singular Value Decomposition (SVD)[J]. Journal of Northeast Normal University (Natural Science), 2006, 38(3): 36-39. (in Chinese)

[4] Deshpande A, Vempala S. Adaptive sampling and fast low-rank matrix approximation[C]// International Conference on Approximation Algorithms for Combinatorial Optimization Problems, and, International Conference on Randomization and Computation. Springer-Verlag, 2006:292-303.

[5] Williams C K I, Seeger M. The Effect of the Input Density Distribution on Kernel-based Classifiers[C]// Seventeenth International Conference on Machine Learning. Morgan Kaufmann Publishers Inc. 2000:1159-1166.

[6] Williams C K I, Seeger M. Using the Nyström method to speed up kernel machines[C]//Advances in neural information processing systems. 2001: 682-688.

[7] Drineas P, Mahoney M W. On the Nyström method for approximating a Gram matrix for improved kernel-based learning[J]. journal of machine learning research, 2005, 6(Dec): 2153-2175.

[8] Boutsidis C, Woodruff D P. Optimal CUR matrix de-

 DOI: https://doi.org/10.26549/met.v3i1.1185

compositions[J]. SIAM Journal on Computing, 2017, 46(2): 543-589.

[9] Anand R, Jeffrey D U. Mining of massive datasets[EB/OL]. (2011-01-03)[2016-03-07]. http://infolab. stanford, edu/~ ullman/mmds/book, pdf.

[10] Drineas P, Mahoney M W, Muthukrishnan S. Relative-error CUR matrix decompositions[J]. SIAM Journal on Matrix Analysis and Applications, 2008, 30(2): 844-881.

[11] Weimer M, Karatzoglou A, Smola A. Improving maximum margin matrix factorization[J]. Machine Learning, 2008, 72(3): 263-276.

[12] Chu M T, Lin M M. Low-dimensional polytope approximation and its applications to nonnegative matrix factorization[J]. SIAM Journal on Scientific Computing, 2008, 30(3): 1131-1155.

[13] Ocepek U, Rugelj J, Bosnić Z. Improving matrix factorization recommendations for examples in cold start[J]. Expert Systems with Applications, 2015, 42(19): 6784-6794.

[14] Chickering D M, Heckerman D. Fast learning from sparse data[C]// Fifteenth Conference on Uncertainty in Artificial Intelligence. Morgan Kaufmann Publishers Inc. 1999:109-115.

[15] Barlaud M, Solé P, Gaidon T, et al. Pyramidal lattice vector quantization for multiscale image coding[J]. IEEE Transactions on Image Processing, 1994, 3(4): 367-381.

[16] Wallace G K. The JPEG still picture compression standard[J]. IEEE transactions on consumer electronics, 1992, 38(1): xviii-xxxiv.

DOI: https://doi.org/10.26549/met.v3i1.1185

SYNERGY PUBLISHING PTE. LTD.

Modern Electronic Technology

https://ojs.s-p.sg/index.php/met

ARTICLE

Boundary Estimation in Annular Two-Phase Flow Using Electrical Impedance Tomography with Particle Swarm Optimization

Rongli Wang*

Department of Physics Science and Technology, Kunming University, Kunming, Yunnan, 650214, China

ARTICLE INFO

Article history
Received: 19 November 2018
Revised: 27 March 2019
Accepted: 8 April 2019
Published Online: 16 April 2019

Keywords:
Electrical impedance tomography
Meshless method
Improved boundary distributed source method
Particle swarm optimization
Annular two-phase flow

ABSTRACT

In this study we consider the boundary estimation of annular two-phase flow in a pipe with the potential distribution on the electrodes mounted on the outer boundary of the pipe, by taking use of electrical impedance tomography (EIT) technique with the numerical solution obtained from an improved boundary distributed source (IBDS) method. The particle swarm optimization (PSO) is used to iteratively seek the boundary configuration. The simulation results showed that PSO and EIT technique with numerical solution obtained from IBDS has been successfully applied to the monitoring of an annular two-phase flow.

1. Introduction

Due to its applications in industry, annular two-phase flow has drawn a lot of attentions in the last decades.[1-3] For annular two-phase flows, the boundary between the liquid and gas phase in the channel is an important aspect for their description. Electrical impedance/resistance tomography (EIT/ERT) is a kind of non-intrusive technique for flow visualization, which has been applied to monitor the multi-phase flow process by many researchers.[2-8] In EIT, a set of electrical currents is injected through a trail of electrodes attached on the boundary of the object and the voltages are measured on the electrodes. Then, with the relationship between the measured voltages and the injected currents the electrical conductivity distribution in the object is reconstructed.

The Finite Element Method (FEM) and Boundary Element Method (BEM) may be the most well-known numerical methods based on mesh for solving EIT forward problems. In contrast, to avoid the disadvantages of numerical methods based on mesh, a new class of numerical methods has been developed only based on a set of nodes without the need for any mesh, called Meshless (or meshfree) Methods (MMs). Many MMs have been proposed and achieved remarkable progress over the last decades.[9-13] In 2013, based on boundary distributed source (BDS)

**Corresponding Author:*
Rongli Wang,
Kunming University, No. 2 Puxin Road, Guandu District, Kunming, Yunnan, 650214, China;
E-mail:mouse_ph@126.com.

Fund Project:
This work was supported by Yunnan Provincial Science and Technology Department (2014FD038) and Program for Innovative Research Team (in Science and Technology) in University of Yunnan Province (IRTSTYN, 2014GXCXTD1).

 DOI: https://doi.org/10.26549/met.v3i1.1228

method, Kim[14,15] suggested an improved boundary distributed source (IBDS) method, which was considered to be efficient to meet the requirements of high precision for the forward problems of EIT.

Particle swarm optimization (PSO) is a parallel evolutionary computation technique based on the social behavior metaphor, which was proposed by Kennedy and Eberhart.[16, 17] Ijaz et al.[5] employed the PSO for the boundary estimation of an elliptic region using ERT, while this work was based on FEM solution of the forward problem. In 2008, Park et al.[6] reported their work about the monitoring of a radioactive waste separation process by taking use of PSO algorithm based on the analytical solution of EIT problem for concentric cases.

In this study, the IBDS is adopted for the EIT forward problem, and the PSO is employed to seek the boundary configuration of gas phase in an annular flow. The final goal of this study is to estimate the boundary between water phase and gas phase in a pipe with the potential distribution measured on the electrodes mounted on the outer surface of the pipe.

2. Mathematic Model of EIT

The cross section of our mathematic model using in EIT is shown in Figure 1, where σ_b is the conductivity of the water region (background), and u_b the potential distribution of the water region, σ_a the conductivity of the air region and u_a the potential distribution of the air region, respectively. The radius of the pipe is R_1, the radius of the air region is R_2, the relative radius $\rho=R_2/R_1$, and the air core located at (x_D, y_D).

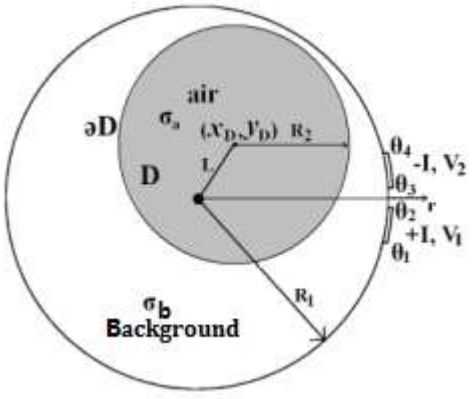

Figure 1. Cross section of the two-phase flow in a pipe with 2 electrodes attached on the boundary

The potential distribution in the subject satisfies the following equation:

$$\nabla\cdot\sigma\nabla u = 0 \tag{1}$$

and the following boundary conditions:

$$\int_{e_l}\sigma\frac{\partial u}{\partial \nu}dS = I_l,\ (x,y)\in e_l,\ l \quad 1,2, \quad ,L \tag{2}$$

$$\sigma\frac{\partial u}{\partial \nu}=0,\ (x,y)\in\partial\Omega\setminus\bigcup_{l=1}^{L}e_l. \tag{3}$$

$$u+z_l\sigma\frac{\partial u}{\partial \nu}=U_l,\ (x,y)\in e_l,\ \ l=1,2,\cdots,L, \tag{4}$$

$$\sum_{l=1}^{L}I_l=0 \text{ and } \sum_{l=1}^{L}U_l=0 \tag{5}$$

where ν is the outward normal unit vector on the boundary, $|e_l|$ is the area of the l th electrode, I_l is the current applied to the l th electrode e_l, z_l is the effective contact impedance, U_l is the measured voltage on the l th electrode and L is the number of electrodes.

3. IBDS Method for EIT Forward Problem

Based on the IBDS formulations,[14,15] the potential distribution and its normal derivative on the background $\Omega\setminus\bar{D}$ and on the inclusion D can be expressed as,

$$u_b(p)=\sum_{j=1}^{M}\tilde{G}(p,p_j)\mu_j^b \text{ and } q_b(p)=\sum_{j=1}^{M}\tilde{Q}(p,p_j)\mu_j^b \tag{6}$$

$$u_a(p)=\sum_{j=1}^{M_D}\tilde{G}(p,p_j)\mu_j^a \text{ and } q_a(p)=\sum_{j=1}^{M_D}\tilde{Q}(p,p_j)\mu_j^a \tag{7}$$

Where p is the field point, p_j are the source points, μ_j^b and μ_j^a are the source densities on the boundaries. And the diagonal elements for the Neumann boundary condition are expressed as:

$$\tilde{Q}(p_j,p_j)\cong-\frac{1}{l_j}\sum_{i=1,i\neq j}^{M}\tilde{Q}(p_i,p_j)l_i \tag{8}$$

Thus, the EIT boundary conditions and interfacial conditions can be rewritten as

$$q_b(p_i)=\sum_{j=1}^{M}\tilde{Q}(p_i,p_j)\mu_j^b=0 \text{ for } p_i\in\partial\Omega_G \tag{9}$$

$$\int_{e_l}\sigma_b q_b(p)dS=I_l \text{ for } l=1,2,\cdots,L \tag{10}$$

$$u_b(p_i)+z_l\sigma_b q_b(p_i)=U_l \text{ for } p_i\in e_l \text{ and } l=1,2,\cdots,L \tag{11}$$

$$u_b(p_i)=u_a(p_i) \text{ and } q_b(p_i)=-\kappa q_a(p_i) \text{ for } p_i\in\partial\Omega_D \tag{12}$$

Where $\kappa=\sigma_a/\sigma_b$.

DOI: https://doi.org/10.26549/met.v3i1.1228

Integrating equation (12) over an electrode and combining equations (8), (9), and (11) we can have

$$\left[\tilde{G}_{EE}\mu_E^b+\tilde{G}_{EG}\mu_G^b+\tilde{G}_{ED}\mu_D^b\right]+\sigma_b\tilde{D}(z_l)\left[\tilde{Q}_{EE}\mu_E^b+\tilde{Q}_{EG}\mu_G^b+\tilde{Q}_{ED}\mu_D^b\right]=C_U U \tag{13}$$

Where

$$\tilde{G}_{IJ}=\tilde{G}(p_i,p_j)\ \text{ for }\ p_i\in\partial\Omega_I,\ p_j\in\partial\Omega_J\ \text{ and }\ I,J\in\{E,G,D\} \tag{14}$$

$$\tilde{D}(z_l)=\text{diag}[z_l(p_1),z_l(p_2),\ldots z_l(p_{M_E})]\otimes I_{m_E}\in\Re^{M_E\times M_E} \tag{15}$$

$$C_U=\text{eye}(L)\otimes\text{ones}(M_E,1) \tag{16}$$

From the insulation condition and interfacial condition, we have

$$\tilde{Q}_{GE}\mu_E^b+\tilde{Q}_{GG}\mu_G^b+\tilde{Q}_{GD}\mu_D^b=0 \tag{17}$$

$$\tilde{G}_{DE}\mu_E^b+\tilde{G}_{DG}\mu_G^b+\tilde{G}_{DD}\mu_D^b=\tilde{G}_{DD}\mu^a \tag{18}$$

$$\tilde{Q}_{DE}\mu_E^b+\tilde{Q}_{DG}\mu_G^b+\tilde{Q}_{DD}\mu_D^b=-\kappa\tilde{Q}_{DD}\mu^a \tag{19}$$

Integrating the boundary condition and imposing the applied current, we have

$$\frac{1}{|e_l|}\int_{e_l}u_b(p)dS+\frac{z_l}{|e_l|}I_l=U_l\ \text{ for }\ l=1,2,\cdots,L \tag{20}$$

$$\bar{G}_{LE}\mu_E^b+\bar{G}_{LG}\mu_G^b+\bar{G}_{LD}\mu_D^b+D(z_l/|e_l|)\tilde{I}=U=N\beta \tag{21}$$

$$\begin{aligned}U=N\beta&=N(N^TN)^{-1}N^T\left[\bar{G}_{LE}\mu_E^b+\bar{G}_{LG}\mu_G^b+\bar{G}_{LD}\mu_D^b+D(z_l/|e_l|)\tilde{I}\right]\\&=\tilde{N}\left[\bar{G}_{LE}\mu_E^b+\bar{G}_{LG}\mu_G^b+\bar{G}_{LD}\mu_D^b+D(z_l/|e_l|)\tilde{I}\right]\end{aligned} \tag{22}$$

Where $N_U=\left[\text{ones}(1,L-1);-\text{eye}(L-1)\right]$ and $\beta\in\Re^{(L-1)\times 1}$.

Thus the IBDS formulation of the EIT becomes

$$\begin{aligned}&\left[\tilde{G}_{EE}+\sigma_b\tilde{D}(z_l)\tilde{Q}_{EE}\right]\mu_E^b+\left[\tilde{G}_{EG}+\sigma_b\tilde{D}(z_l)\tilde{Q}_{EG}\right]\mu_G^b+\left[\tilde{G}_{ED}+\sigma_b\tilde{D}(z_l)\tilde{Q}_{ED}\right]\mu_D^b\\&=C_U\tilde{N}\left[\bar{G}_{LE}\mu_E^b+\bar{G}_{LG}\mu_G^b+\bar{G}_{LD}\mu_D^b+D(z_l/|e_l|)\tilde{I}\right]\end{aligned} \tag{23}$$

$$\begin{aligned}&\left[\tilde{G}_{EE}+\sigma_b\tilde{D}(z_l)\tilde{Q}_{EE}-C_U\tilde{N}\bar{G}_{LE}\right]\mu_E^b+\left[\tilde{G}_{EG}+\sigma_b\tilde{D}(z_l)\tilde{Q}_{EG}-C_U\tilde{N}\bar{G}_{LG}\right]\mu_G^b\\&+\left[\tilde{G}_{ED}+\sigma_b\tilde{D}(z_l)\tilde{Q}_{ED}-C_U\tilde{N}\bar{G}_{LD}\right]\mu_D^b=C_U\tilde{N}D(z_l/|e_l|)\tilde{I}\end{aligned} \tag{24}$$

We can express equation (24) as

$$V_{EE}\mu_E^b+V_{EG}\mu_G^b+V_{ED}\mu_D^b=C_U\tilde{N}D(z_l/|e_l|)\tilde{I} \tag{25}$$

Where

$$V_{EE}=\tilde{G}_{EE}+\sigma_b\tilde{D}(z_l)\tilde{Q}_{EE}-C_U\tilde{N}\bar{G}_{LE} \tag{26}$$

$$V_{EG}=\tilde{G}_{EG}+\sigma_b\tilde{D}(z_l)\tilde{Q}_{EG}-C_U\tilde{N}\bar{G}_{LG} \tag{27}$$

$$V_{ED}=\tilde{G}_{ED}+\sigma_b\tilde{D}(z_l)\tilde{Q}_{ED}-C_U\tilde{N}\bar{G}_{LD} \tag{28}$$

$$\bar{G}_{LJ}=\frac{s_E}{|e|}\left[I_L\otimes ones(1,m_E)\right]\tilde{G}_{EJ}=A\tilde{G}_{EJ}\ \text{ for }\ J\in\{E,G,D\} \tag{29}$$

Finally, the system equations can be written as

$$\begin{bmatrix}V_{EE}&V_{EG}&V_{ED}&0\\\tilde{Q}_{GE}&\tilde{Q}_{GG}&\tilde{Q}_{GD}&0\\\tilde{G}_{DE}&\tilde{G}_{DG}&\tilde{G}_{DD}&-\tilde{G}_{DD}\\\tilde{Q}_{DE}&\tilde{Q}_{DG}&\tilde{Q}_{DD}&\kappa\tilde{Q}_{DD}\end{bmatrix}\begin{bmatrix}\mu_E^b\\\mu_G^b\\\mu_D^b\\\mu_D^a\end{bmatrix}=\begin{bmatrix}C_U\tilde{N}D(z_l/|e_l|)\tilde{I}\\0\\0\\0\end{bmatrix} \tag{30}$$

When the parameter set X=[x_D, y_D, ρ] is given, the voltages on the electrodes can be calculated from Eqs. (4-7). In the EIT forward problem considered in this paper, the parameters is not known and it should be estimated based on the injected currents and the measured voltage data V_m (l=1,2,…,M). So the problem to be solved is to identify the unknown parameter set [x_D, y_D, ρ] which minimize the difference between the measured voltages V^l induced by the l-th current pattern and the calculated voltage U^l. The object function to be minimized is defined as

$$\psi=\sum_{l=1}^{L}\frac{\left\|V^l-U^l\right\|}{\left\|V^l\right\|} \tag{31}$$

 DOI: https://doi.org/10.26549/met.v3i1.1228

4. PSO Algorithm

The PSO algorithm is initialized with a set of random particles. Each individual in the particle swarm is composed of three K-dimensional vectors. These are the current position $\vec{x}_i$, the previous best position $\vec{p}_i$, and the velocity $\vec{v}_i$. The original process for implementing PSO is as following:[16, 17]

(1) Initialize a set of random particles with random $\vec{x}_i$ and $\vec{v}_i$.

(2) Start loop

(3) For each particle, evaluate the desired optimization fitness function.

(4) Compare particle's fitness evaluation with its $pbest_i$. If current value is better than $pbest_i$, then update $pbest_i$ to the current value, and $\vec{p}_i$ equal to $\vec{x}_i$.

(5) Update $\vec{x}_i$ and $\vec{v}_i$ according to the following equation:

$$\begin{cases} \vec{v}_i \leftarrow c \otimes \vec{v}_i + b_1 \otimes w_1 \otimes (\vec{p}_{Lbest} - \vec{x}_i) + b_2 \otimes w_2 \otimes (\vec{p}_{Gbest} - \vec{x}_i) \\ \vec{x}_i \leftarrow \vec{x}_i + \vec{v}_i \end{cases} \tag{32}$$

(6) If the maximum number of iterations is reached, then exit loop.

In equation (32), w_1 and w_2 are random numbers selected in the range [0,1], and p_{Lbest} denoted the local best solution of the current particle, while p_{Gbest} denoted the global best solution in the whole population. In this paper, we set c=0.6 and $b_1=b_2=1.7$ as derived by Trelea [18].

5. Numerical Results

In the simulation, suppose 4 electrodes were attached on the boundary. Three current patterns [1, -1, 0, 0], [1, 0, -1, 0] and [1, 0, 0, -1] with the magnitude I_m are used.

In practically, considered the noise of the measured voltages, our data calculated from IBDS consider the measurement error as following:

$$V_{meas} = V(1 + \varepsilon_n)$$

Where the measurement error ε_n is assumed to be Gaussian with zero mean. In the PSO algorithm, 10 particles are used, and the maximum number of iterations is 200.

Two numerical examples are simulated in this work, $X=[x_D, y_D, \rho]=[0, -0.05, 0.9]$ and $X=[x_D, y_D, \rho]=[-0.3, -0.05, 0.6]$, the conductivity of water σ_b is set as 1/300 $S\cdot cm^{-1}$, and the conductivity of air $\sigma_a=0$. For each case, different percentage of noise are concerned: with 0% noise, 1% noise and 5% noise, respectively.

Table 1 shows the numerical results for the two cases. From the parameters of the numerical examples it can be seen that the PSO technique estimates the location and radius of the air core quite well. The estimated parameters of the two examples are the same as the true value and the object function ψ is smaller than 10^{-5} without noise. For the other cases with noise, the location of the air core is estimated well, and the object function ψ is proportional to the relative noise.

Table 1. Parameters of the numerical examples

True value			Noise	Estimated value			ψ
xD	yD	ρ		xD	yD	ρ	
0	-0.05	0.9	0%	0.0000	-0.0500	0.9000	0.0000
			1%	0.0000	-0.0494	0.9011	0.0442
			5%	0.0000	-0.0485	0.9032	0.2101
-0.3	-0.05	0.6	0%	-0.3000	-0.0500	0.6000	0.0000
			1%	-0.2981	-0.0497	0.6031	0.0490
			5%	-0.2890	-0.0479	0.6132	0.2417

6. Conclusion

In this study we consider the monitoring of an annular two-phase flow using EIT technique. The numerical solution of the forward EIT problem with eccentric cases is derived by using IBDS. The PSO algorithm is employed to estimate the center location and radius of the air core in water-air two-phase flow with the voltage on the electrodes attached on the outer boundary of the pipe, by minimizing a cost functional with the analytical solution. The simulation results showed that PSO and EIT technique has been successfully applied to the monitoring of an annular two-phase flow.

References

[1] A. Cioncolini, J. R. Thome and C. Lombardi, Algebraic turbulence modeling in adiabatic gas-liquid annular two-phase flow[J]. International Journal of Multiphase Flow, 2009, 35(6):580-596.

[2] F. Dong, Y.B. Xu, L.J. Xu, L. Hua, and X.T.Qiao, Application of dual-plane ERT system and cross-correlation technique to measure gas–liquid flows in vertical upward pipe[J]. Flow Measurement and Instrumentation, 2005, 16(2-3):191-197.

[3] H. J. Jeon, B. Y. Choi, M. C. Kim, K. Y. Kim and S. Kim, Phase Boundary Estimation in Two-Phase Flows with Electrical Impedance Imaging Technique[J]. International Communications in Heat and Mass Transfer, 2004, 31(8):1105-1114.

[4] M. C. Kim, K. Y. Kim, K. J. Lee, Y. J. Ko and S. Kim, Electrical impedance imaging of phase bound-

DOI: https://doi.org/10.26549/met.v3i1.1228

ary in two-phase systems with adaptive mesh regeneration technique[J]. International Communications in Heat and Mass Transfer, 2005, 32(7):954-963.

[5] U. Z. Ijaz, A. K. Khambampati, M. C. Kim, S. Kim, J. S. Lee and K. Y. Kim, Particle swarm optimization technique for elliptic region boundary estimation in electrical impedance tomography[J]. AIP Conference Proceedings, 2007, 914:896-901.

[6] B. G. Park, J. H. Moon, B. S. Lee and S. Kim, An electrical resistance tomography technique for the monitoring of a radioactive waste separation process[J]. International Communications in Heat and Mass Transfer, 2008, 35(10):1307-1310.

[7] D. L. Georgea, J. R. Torczynskia, K. A. Shollenbergera, T. J. O'Herna, and S. L. Ceccio, Validation of electrical-impedance tomography for measurements of material distribution in two-phase flows[J]. International Journal of Multiphase Flow, 2000, 26(4):549-581.

[8] Z. Meng, Z. Huang, B. Wang, H. Ji, H. Li, and Y. Yan, Air-water two-phase flow measurement using a Venturi meter and an electrical resistance tomography sensor[J]. Flow Measurement and Instrumentation, 2010, 21(3):268-276.

[9] Z. Zhang, P. Zhao, K.Liew , Improved element-free Galerkin method for two-dimensional potential problems[J]. Engineering Analysis with Boundary Elements, 2009, 33(4):547-554.

[10] Y. Gu, G. Liu, Meshless Methods Coupled with Other Numerical Methods[J]. Tsinghua Science and Technology, 2005, 10(1):8-15.

[11] M. Jalaal, S. Soheil, G. Domairry, et al, Numerical simulation of electric field in complex geometries for different electrode arrangements using meshless local MQ-DQ method[J]. Journal of Electrostatics, 2011, 69(3):168-175.

[12] T. Belytschko et al., Meshless methods: an overview and recent developments[J]. Computer Methods in Applied Mechanics and Engineering, 1996, 139(1-4):3-47.

[13] K.Chen, J.Kao, J. Chen, D. Young, Mu, Regularized meshless method for multiplyconnected-domain Laplace problems[J]. Engineering Analysis with Boundary Elements, 2006, 30(10):882-896.

[14] S. Kim, An improved boundary distributed source method for two-dimensional Laplace equations[J]. Engineering Analysis with Boundary Elements, 2013, 37:997-1003.

[15] S. Kim, R. Wang et al. An improved boundary distributed source method for electrical resistance tomography forward problem[J]. Engineering Analysis with Boundary Elements, 2014, 44:185-192.

[16] J. Kennedy and R. Eberhart, Particle swarm optimization[C]. in: Proceedings of IEEE International Conference on Neural Networks, Piscataway, NJ, 1995, 1942-1948.

[17] R. Eberhart and J. Kennedy, A New Optimizer Using Particle Swarm Theory[C]. Sixth International Symposium on Micro Machine and Human Science, 1995, 39-43.

[18] I. C. Trelea, The particle swarm optimization algorithm: convergence analysis and parameter selection[J]. Information Processing Letters, 2003, 85(6):317-325.

 DOI: https://doi.org/10.26549/met.v3i1.1228

SYNERGY PUBLISHING PTE. LTD.

Modern Electronic Technology

https://ojs.s-p.sg/index.php/met

ARTICLE

Study on Railway Marshalling Scheduling Model and Algorithm of Enterprise Station

Jiawei Wen, Gang Lu*, Nanshan Xu

Beijing University of Chemical Technology, Beijing, 100029, China

ARTICLE INFO

Article history
Received: 22 November 2018
Revised: 28 March 2019
Accepted: 8 April 2019
Published Online: 16 April 2019

Keywords:
Station railway
Marshalling algorithm
Greedy algorithm
Scheduling rule method library

ABSTRACT

Railway marshalling transportation is a crucial part of enterprise production supply chain, with the development of national economy; enterprises face more and more pressure on station railway marshalling operation. Realizing enterprise railway dispatching plan automatically by computer, which can improve the level of the station scheduling and transport efficiency, at the same time can reduce the scheduling cost. Based on the basic rules of marshalling and dispatching of railway freight trains at enterprise stations, this paper investigates the site of special railway line at enterprise stations and establishes the space of dispatching state and regulation base according to the actual situation. The information feedback model is designed according to the train information, carriage information and real-time information of the track of the station. Based on the analysis of the railway regulation and the demand of the station, establish the scheduling rule method library. Based on the state space and feedback model of the station, using the scheduling rule method library, this paper designs an enterprise railway automatic marshalling algorithm with a certain universality, and realizes automatic train marshalling and scheduling operation. Considering the economic benefit of the station and the efficiency of the marshalling model, this paper introduces the time cost function and applies the improved greedy algorithm to optimize the automatic marshalling model, realizing the optimal marshalling of railway station in a short time.

**Corresponding Author:*
Gang Lu,
Master's tutor and lecturer, College of Information Science and Technology, Beijing University of Chemical Technology, No. 15 North Third Ring Road, Chaoyang District, Beijing, 100029, China;
Email: sizheng@vip.126.com
About other authors:
Jiawei Wen,
master of software engineering, Beijing University of Chemical Technology, No. 15 North Third Ring Road, Chaoyang District, Beijing, 100029, China;
Email: jiaweiwen0204@foxmail.com.
Nanshan Xu,
associate professor, master's tutor, Beijing University of Chemical Technology

DOI: doi.org/10.26549/met.v3i1.1272

1. Introduction

Railway marshalling transportation is responsible for the incoming of raw materials, the transportation of semi-finished product and the delivery of finished products, and a lot of other works. Therefore, railway marshalling and dispatching is an important infrastructure to ensure the normal operation of enterprises. Because the station railway is generally small in scale and the cost of using the existing railway intelligent dispatching system is high, most railway enterprises in China still rely on the dispatcher to manually compile the marshalling scheduling plan, which causes a huge gap with the advanced national intelligent railway network. But with the development of national economy, enterprise station railway faces more and more pressure. As the railway freight volume of station increases, the need for marshalling and scheduling becomes more and more frequent. As the same time, job types of scheduling techniques are increasing and require greater flexibility. For enterprises, the operation of station railway marshalling not only needs to meet the planned production and transportation demand, but also needs to consider reducing the cost of the dispatching process, such as labor cost and energy consumption cost, which is great significance for reducing the transportation cost of enterprises and promoting environmental protection and energy conservation. Under the constraints of enterprise station railway scale and production cost, the existing intelligent railway dispatching system can hardly be applied directly to enterprise railway. Train scheduling and marshalling problem is a typical n-p problem. The conventional design idea is solved by mathematical modeling and genetic algorithm. In the field of mathematical modeling, Li[1] proposed a train control system based on global information feedback model for train scheduling. Krasemann[2] and He[3] respectively apply the greedy algorithm to reduce interference and avoid train interference, so as to realize rapid rescheduling of trains. By introducing genetic algorithm, Rui[4] solved the fuzzy scheduling problem in railway management system.

This paper designs a kind of general marshalling scheduling algorithm for enterprise station railway and realizes the automatic compilation of enterprise railway scheduling plan by computer. This algorithm cannot only shorten the time of planning, improve the quality of the planning, reduce the burden of staff, but also to improve the level of the station scheduling in practical transport production and the efficiency of enterprise railway transportation has very important significance.

1.1 Background Knowledge

Station railway: also known as station yard, it refers to all railway tracks, including arrival and departure yard, parking yard, throat area, overhaul area, pulling out line, loading and unloading walking line and so on.[5]

Disassembly: decompose the trains according to the different demand of carriage distribution.

Distribution: according to the related requirements of the station planning sheet, in combination with the train arrival at the station, select the corresponding train group to carry out the disassembly operation, and arrange enough carriages for the marshalling departure in time.

Marshalling: according to the planned requirements reorganize the trains.

Stage plan: according to the station equipment capacity, production status and the state of the railway approved vehicles, pre-prepared the station equipment application program within a certain period.

1.2 The Research Target

Disassembly, distribution and marshalling are the core processes of station train marshalling and scheduling. The common goal of the three processes is to organize a new train as soon as possible and prepare for departure at the minimum cost on the premise of meeting the planning requirements [6]. Because the train scheduling process involves a large number of variables and multiple rules, the rules should be transformed into constraints when modeling, so the train marshalling scheduling problem is essentially a large-scale combinatorial optimization problem. This paper mainly studies the following problems:

Design the automatic train marshalling scheduling model. According to the real-time status of the station, the computer can automatically compile the scheduling scheme, and the feasible marshalling meeting the planning requirements is obtained.

The marshalling scheduling model is universal and flexible, which can be applied to different railway stations of different enterprises and can be used to deal with emergency priorities.

Considering the economic benefit and cost of the enterprise station, the automatic marshalling model is optimized so that the obtained scheduling scheme has the shortest marshalling time and the minimum starting cost.

In the design of marshalling scheduling model, the scale of data processing needs to be taken into account to avoid data explosion, reduce the amount of data processing and improve the solution speed under the premise of ensuring the optimal solution.

2. Mathematical Models

2.1 Train State Model

When the stage plan starts, there are n carriages in the sta-

 DOI: doi.org/10.26549/met.v3i1.1272

tion, and the status of the train in the station is shown in list A, A=[S(1), S(2)… S(n)]. S(i) represents the full state of a single carriage, S(i)=[S_w, S_c, S_p, S_t, S_l, S_n, S_o, S_a].

S_w, S_c, S_p and S_a represent the carriage wagon number, carriage category, carriage commodity and carriage attribution respectively. Each carriage has a fixed wagon number and place of attribution, and can only carry a specific commodity. In the same way each commodity must be carried by a specific category of carriage. S_t and S_l indicate the train's position and state, S_t indicates the parking track of the carriage, and S_l indicates the positioning of the carriage on the corresponding track. S_n refers to the effective state of the train, and S_n=1, 0 is set to indicate whether there is any follow-up plan for the carriage. S_o represents the train's working state, S_o=1, 2, 3 respectively represent the three working states of railway carriages in the station during the stage planning period. When S_o=1, the carriage is in the existing state, which means that the carriage has completed all the foreordination tasks and is placed on the respective track, which can be directly invoked. When S_o=2, the carriage is in the waiting loading and unloading state, which means that the carriage has arrived at the station, and the train information has been entered through the loading and unloading inspection, waiting for the unloading operation after the disassembly. When S_o=3, the carriage is in running state, which means that the carriage is about to arrive at the station according to the railway operation diagram and has been registered on the dispatch schedule.

2.2 Orbital State Model

When the stage plan starts, there are m orbits in the station, and the status of the orbit in the station is shown in list B, B = [P(1), P(2)... P(m)]. P(i) represents the full state of a single orbit, P(i) = [P_t, P_w, P_f].

P_t represents the orbit name, P_w represents the carriage capacity of the track, number each track from 1 to P_w, and the carriage can stop at the corresponding sign. F is the orbit function set of the station. P_f={1,2,3,4,5} represents the five types of functions of the station's track: arrival and traction marshalling line, preparatory emergency task line, parking traction line, loading line and unloading line.

2.3 The Introduction of Time Cost

2.3.1 Time Cost of Scheduling Operations[7]

Suppose the marshalling waiting time of the carriage is T_w and the stage planning cycle is T_D. The marshalling waiting time of the carriage under different working conditions is as follows:

Existing trains:

$$T_W = t_{jt} + t_{bz} + \triangle t \tag{1}$$

Arrival waiting for loading/unloading trains:

$$T_W = t_{jt} + t_{zx} + t_{bz} + \triangle t \tag{2}$$

Running trains:

$$T_W = T_{dd} + t_{jt} + t_{zx} + t_{bz} + \triangle t \tag{3}$$

t_{jt} refers to the time when the carriage hangs and disconnects from the original track, t_{bz} refers to the time when the carriage is marshaled in a dispatch operation, $\triangle$ t refers to the waiting time caused by equipment or human factors. t_{zx} refers to the loading and unloading operation time. T_{dd} is the estimated arrival time of the scheduled train.

2.3.2 Orbital Time Cost

The list L represents the connectivity relationship between the different orbits, L= [T(1), T(2)…T(n)], T(i)= [T_l, T_r, T_w], T_l and T_r are two connected orbits, and T_w is the time cost of moving trains between T_l and T_r. To sum up, the time cost of completing all the scheduling shall not exceed the phase scheduling cycle, the scheduling must be completed within the specified time with constraints:

$$T_D \geq \sum T_W \tag{4}$$

The goal of optimal marshalling scheduling is to satisfy the phase plan while achieving the minimum time cost.

$$\left(\sum T_w\right)_{\min} \tag{5}$$

3. The Scheduling Rule Method Library

Due to the considerations of production products, geographical location and other factors, the enterprise station railways often have great uniqueness under the principle of abiding by the national railway scheduling rules, while the factors of marshalling and scheduling among different stations are also very different. The system universality can be greatly improved by establishing a database of scheduling rules, encapsulating each general scheduling rule independently and making calls based on different station situations [8]. By using scheduling rules, the generation of invalid scheduling schemes can be avoided and the amount of data processing can be reduced.

3.1 General Constraint

3.1.1 Security Constraint

There is only one locomotive activity in the station at any

DOI: doi.org/10.26549/met.v3i1.1272

time. Only one scheduling job can be performed at the same time, which avoids the interference between scheduling operations and ensures the safety of station scheduling.

3.1.2 Anti-pollution Constraint

In order to ensure the safety of commodities and avoid pollution, a carriage only transports one commodity.

3.2 The Selection Rule of the Carriage

The purpose of the rule is to select the appropriate carriage from all carriages of the station by screening the commodity name Rc and quantity of the carriage Rn. Initialize the station status space, get all the train list A, A=[S (1), S (2)… S (n)], according to this algorithm the whole suitable carriage list A_0 can be obtained. The algorithm pseudocode is as follows.

Table 1. Algorithm pseudocode of selecting the fitting-carriage

```
Algorithm 1:Select the fitting-carriage
Input: A=[S(1), S(2)… S(n)], S(i)=[Sw, Sc, Sp, St, Sl, Sn, So, Sa], Rc, Rn
Output: the fitting-carriage list A0
1 A1←[], A2←[], A0←[]
2 for S(i) in A do
3    if S(i). Sc=Pc then
4       A1.append(S(i))
5    end
6 end
7 if length(A1)≥Rn then
8    for S(j) in A1 do
9       if S(j). Sn=0 then
10         A2.append(S(j))
11      end
12   end
13   if length(A2)≥Rn then
14      A0←A2
15   else
16      A0←A1
17   end
18   Output A0
19 else
20   Output 'The stage plan cannot be completed'
21 end
```

3.3 The Read Rule of Emergency Priority Plan

Set the priority symbol R_p, R_p =0, 1, for each plan on the stage plan list, if there is an emergency priority plan, R_p=1, it is preferred to carry out the plan scheduling. The preparatory emergency task line is used as the target marshalling track, which is not subject to the lower limit of the marshalling starting load.

3.4 The Parking Rule of the Disintegrating Train

In the process of disassembly, it is often necessary to make temporary movement of the unqualified carriages. According to the functional definition of the track, only the arrival traction marshalling line and parking traction line can be temporarily scheduled and parked. The purpose of the rule is to obtain all temporary orbits that satisfy the functional type and are currently empty and put them in the list B*. Initialize the station status space, get the entire train list A, A=[S(1), S(2)… S(n)], get the entire orbit list B, B=[P(1), P(2)... P(m)]. The algorithm pseudocode is as follows.

Table 2. Algorithm pseudocode of selecting fit temporary orbit

```
Algorithm 2:Select fit temporary orbit
Input: A=[S(1), S(2)… S(n)], B = [P(1), P(2)... P(m)]
Output: the fit temporary orbit list B*
1 B1←[], B2←[],B3←[]
2 for S(i) in A do
3    B1.append(S(i). St)
4 end
5 B2←CB(B1)
6 for S(j) in B do
7    if Pf= 1|| Pf=3 then
8       B3.append(S(j))
9    end
10 end
11 B*← B2∩B3
12 Output B*
```

3.5 Load Constraint of Locomotive[6]

$$L_f^{\min} \le L(j) \le L_f^{\max}, \forall j \in D \tag{6}$$

$$W_f^{\min} \le W(j) \le W_f^{\max}, \forall j \in D \tag{7}$$

While considering the marshalling time, the economics of scheduling operations should be constrained. In the formula, D denotes the train sets that need to be moved, L is the number of locomotive traction carriages. Formula (6) is the limitation of the number of carriages towed by locomotives. The main objective of the constraint is to prevent the enterprise from excessively pursuing the shortest scheduling time while ignoring the economic benefits. This constraint is mainly used to limit the number of carriages of trains that have been marshalled and are waiting to leave. The number of carriage per departure at the enterprise station shall reach a certain lower limit, but not exceed the carrying capacity of the locomotive at the same time.

Formula (7) is the limitation of the total weight of the locomotive towed carriage, W is the tractable load of locomotive. This constraint limits the economic benefit and time cost of locomotive departure from the perspective of load. The total weight of the waiting train shall not exceed the traction capacity of the locomotive, but it must meet the lower limit of departure.

 DOI: doi.org/10.26549/met.v3i1.1272

4. Greedy Algorithn Design

Greedy algorithm means that when solving problems, it always makes the best choice in the current situation. The core of the station railway marshalling and dispatching is to find the marshalling scheme with minimum time cost and optimal economic benefits based on the completion of the plan. At the same time, when the number of stations and the number of trains reaches a certain scale, the number of possible scheduling and marshalling schemes will explode, and the introduction of greedy strategy can effectively avoid this situation. In this paper, greedy algorithm is introduced in the selection of carriage, composition of carriage group and the selection of track involved in scheduling. Taking advantage of the greedy algorithm, the optimal solution can be obtained by generating fewer schemes in less time.

4.1 The Application of Greedy Algorithm

4.1.1 The Choice of the Best Carriages

According to the analysis of the waiting time T_w formula of different working states of the carriages, it can be known that the waiting time of the three working states is gradually increased in the existing state, waiting for loading and unloading state and running state, and the shortest waiting time is the carriage in the existing state. According to the screening by scheduling rules, all adaptive carriage list A_0 has been obtained. Greedy algorithm is used to get the optimal carriage list A* the algorithm pseudocode for finding the optimal carriage is as follows.

Table 3. Algorithm pseudocode of selecting the best carriages

```
Algorithm 3:Select the best carriages
Input: A0=[S(1), S(2)… S(m)], S(i)=[Sw, Sc, Sp, St, Sl, Sn, So, Sa], Rn
Output: the best-carriage list A*
1 A*←[]
2 for S(i) in A0 do
3     if S(i). So=1 then
4         A*.append(S(i))
5     end
6 end
7 if length(A*)<Rn then
8     for S(j) in A0 do
9         if S(j). So=2 then
10            A*.append(S(j))
11        end
12    end
13    if length(A*) <Rn then
14        A*←A0
15    end
16    Output A*
17 else
18    Output A*
19 end
```

4.1.2 The Choice of the Best Dispatch Orbit

According to the parking rule of the disintegrating train, select the optimal dispatch channel with the minimum moving cost. However, if there are multiple train disassembly operations in a plan, different orbits may interfere with each other, so this greedy strategy is used for the plan of single disassembly only. The algorithm flow is as follows.

Step 1: Initialize the station status space, get the list L of connected relationships of all tracks in the station, and get the carriage's orbit T_0 which need to move, then according to the parking rule of the disintegrating train get the temporary track list B*.

Step 2: Traverse all orbit in list L. If $T_l = T_0$, or $T_r = T_0$, put all the orbits that are connected to T_0 in list L_1.

Step 3: $L^* = L_1 \cap B^*$. According to the track design rules of the station, there is no unconnected part in the track of the station, so $L^* \neq null$.

Step 4: Iterate through the list L* to find the femoral T_{best} with the minimum T_w moving time cost.

4.1.3 The Choice of the Best Carriage Groups

According to the daily safety regulations of railway stations, carriages parked on each track are connected in a row. In the selection of multiple marshalling carriages, if some adaptive carriages were joined together in a row, the time cost of disassembly, Distribution, and marshalling on these carriages would be greatly reduced. Therefore, when the optimal carriages in list A*connected to form into a group, if the group containing the number of carriages greater than or equal to the planned number R_n of carriages, we will get the optimal cost of marshalling time; because at this point the train needs to carry out the least number of disassembly operations. At the same time, if the first carriage of the group is at the beginning of the track 1 position, the time cost of scheduling will be further reduced. Since there is more than one carriage group that meets the conditions of greedy strategy, all suitable carriage groups are placed in the list G*. The algorithm for finding the best carriage group is as follows.

Step 1: Initialize the station status space, get the best-carriage list A*, and read the stage plan to get the required the required number of carriages R_n.

Step 2: Locating all carriages in A* and get the connected carriage group list G, $G= [g_1, g_2 \ldots g_n]$, $g_i=[S(1), S(2) \ldots S(q)]$.

Step 3: Traverse all carriage groups in list G. If group g_i contains carriages more than or equal to R_n, the corresponding group g_i would be stored in the group list G_1, until the traversal is complete to get the full group list G_1.

DOI: doi.org/10.26549/met.v3i1.1272

Step 4: If $G_1 \neq$null, all groups in list G_1 are traversed. If group g_i contains carriages whose S_l=1, the corresponding group g_i is stored in the best-group list G*, until the traversal is complete to get the full best-group list G*.

Step 5. If group g_i doesn't contain carriages whose $S_{l=}1$, according to choice of the best dispatch orbit, make temporary movement of the unqualified carriages, G*= G_1, and record the time cost T_w.

4.2 Marshalling Algorithm Design

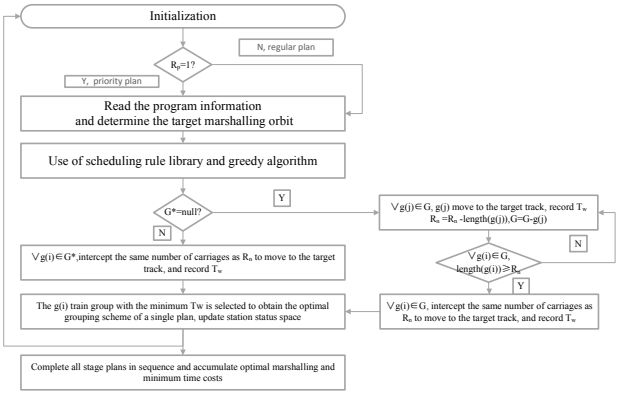

Figure 1. Flowchart of marshalling algorithm

Step 1: Initialization. Initialize the station state space, the orbital list and the phase scheduling plan sheet.

Step 2: Emergency priority planning judgment. Use the traversal scheduling plan sheet. If there is an emergency priority plan in the phase plan table, R_p=1, the emergency plan is prioritized firstly. If not, the regular plan should be marshalled in sequence.

Step 3: Read the program information and determine the target marshalling orbit. In the orbital list B, if there is a regular plan, arbitrarily select the orbit P(i) of P_f=1 as the target marshalling orbital T*. As for emergency priority plans, choose the orbit whose P_f=2 as the target marshalling orbital T*.And read the stage plan to get the required commodity name R_c and the required number of carriages R_n.

Step 4: Use of scheduling rule library and greedy algorithm. According to the choice of the best carriages, get the fitting-carriage list A_0. According to the choice of the best carriages, get the full best-carriage list A*. According to the choice of the best carriage groups, get the best carriage group list G* and the connected carriage group list G.

Step 5: When the list G* is not empty, as for each group g(i) in G*, respectively intercept the same number of carriages as R_n to move to the target track, and record the time cost T_w. The carriage group g(i) with the minimum Tw is selected to obtain the optimal grouping scheme of a single plan, then update station status space.

Step 6: If the list G* is empty, sort the carriage group in list G from large to small, then, each group g(j) in G respectively move to the target track and record the time cost T_w, R_n =R_n -length(g(j)), G=G-g(j). Update the station status space and determine whether the remaining carriage groups can directly meet the planned number. If there is g(i) in G, length(g(i))≥R_n, intercept the same number of carriages as R_n to move to the target track, and record the time cost T_w. These groups have the lowest cumulative time cost are selected to obtain the optimal grouping scheme of a single plan, then update station status space.

Step 7: Sequential read plan, repeat steps 1-6, until all the plan is completed, and record all marshalling time to calculate the least time-consuming marshalling scheme.

4.3 Algorithm Analysis

The algorithm is universal and flexible. In terms of the program design, the track state, the station train state, the track connectivity relationship and the stage schedule can be directly modified, which greatly improves the universality of the model. The emergency plan has been set with a sign, which can be quickly recognized and scheduled.

The concern of this algorithm lies in step 5, 6. For the general enterprise station, the parking of the train carriages should be as neat as possible. For example, after unloading, the carriages will be parked separately according to the name of the product or the place where the carriages belong. And the station should be maintained with enough carriages for daily production and transportation and emergency response. The more standard of the station, the more efficient of the greedy algorithm; If the carriages carrying the same cargo are parked together in an orderly way after loading and unloading, the number of carriages in the list G* can always meet the planned number, and the efficiency of this algorithm will be greatly improved.

5. Experiment and Performance Analysis

This paper takes the railway station of Baling petrochemical supply and Marketing Department of Yueyang city, Hunan province, China as the experimental environment, and conducted the experiment on the stage plan and the state of the field. There are 27 tracks and 41 sets of side connections in the station, and have 67 carriages, 7 stage plans, and 1 available locomotive in the experimental environment. The experimental results of automatic marshalling algorithm based on greedy strategy and scheduling rule base are as follows.

Plan 5 is a priority plan, so it is executed first by the algorithm. It can be seen from the experimental results, there is no big difference between the two methods when

 DOI: doi.org/10.26549/met.v3i1.1272

Table 4. Comparison of experimental results

	Scheduling rule library			Scheduling rule library+ Greedy algorithm			Data processing volume decrease percentage	Percentage decrease in data processing time
	Scheme quantity	Optimal time cost (min)	Solve time (s)	Scheme quantity	Optimal time cost (min)	Solve time (s)		
Plan5	2	40	3.77	2	40	2.31	0%	38.72%
Plan1	1	35	2.66	1	35	2.67	0%	0%
Plan2	9	80	6.91	1	80	2.09	88.89%	69.95%
Plan3	2	45	2.67	2	45	2.64	0%	1.12%
Plan4	22	40	11.87	2	40	6.65	90.91%	43.97%
Plan6	137	80	43.50	48	80	34.58	64.96%	20.45%
Plan7	110	40	50.01	44	40	27.60	60%	44.81%
Total	340	360	122.64	128	360min	64.28	62.35%	47.59%

the carriages are parked neatly and in sufficient quantity on the spot, such as the marshalling of plan 1 and plan 3. When non-marshalling carriages movement is required, greedy algorithm can quickly select temporary track to realize marshalling, such as plan 2 and plan 4. The scheduling algorithm introduced by greedy strategy is better than using only the scheduling rule library. When the number of available carriages is large, but the parking locations are scattered, which cannot meet the planning needs at one time, the running time of automatic marshalling algorithm and the number of schemes generated will increase with the increase of the number of scheduling. At this time in order to avoid the problem of local optimization caused by greedy algorithm, greedy strategy is only used in the choice of temporary dispatch channel, but not in the choice of optimal carriages. At this point, the algorithm still effectively improves the performance, as shown in the experimental results of plan 6 and 7. When the entire schedule is marshaled, there will be interference between different plans, and the algorithm's operation time and data processing amount will increase, but the algorithm still achieves the expected performance. The experimental results show that the designed automatic marshalling strategy can realize the automatic compilation of scheduling plan in a very short time, and get approximate optimal marshalling scheme and the minimum time cost.

6. Conclusion

In this article, through the analysis of enterprise station marshalling scheduling process, determine the scheduling process real-time information, the automatic compilation algorithm of station railway marshalling and dispatching is established. This model is well balanced fast marshalling and optimal time cost contradictions. In this paper, the time cost is used as the index to measure the marshalling scheme. In addition to solving the optimal scheduling scheme, the greedy algorithm reduces the complexity of the algorithm and improves the solving speed. And the economic benefits of the enterprise are guaranteed by multiple constraints of the scheduling rule base. The feasibility and reliability of the model have been verified by practical simulation. The algorithm proposed in this paper is progressive significance to realize automatic scheduling and intelligent marshalling of enterprise stations.

References

[1] Li F, Gao Z, Li K, et al. Efficient scheduling of railway traffic based on global information of train[J]. Transportation Research Part B: Methodological, 2008, 42(10):0-1030.

[2] Krasemann, J. T. Greedy algorithm for railway traffic re-scheduling during disturbances: A Swedish case[J]. IET Intelligent Transport Systems, 2010, 4(4):375-0.

[3] He Z. Research on Improved Greedy Algorithm for Train Rescheduling[C]// Seventh International Conference on Computational Intelligence & Security. IEEE, 2012.

[4] Shi-Wei HE, Rui S , Fang L U, et al. Fuzzy Scheduling Problem with Multi-Processors Using Genetic Algorithm for Railway Management[J]. Journal of Beijing University of Aeronautics and Astronautics (Social Sciences Edition), 2000.

[5]Suixian Z, Yiping L. Railway lines and stations[M]. Southwest Jiaotong University Press, 2006. (in Chinese)

[6] Wuzu W. A Freight Train Marshalling-Scheduling Model and Algorithms[J]. Computer & Digital Engineering, 2009. (in Chinese)

[7] Qingsong S. Study on Automatically Making and Adjusting Stage Plan of the Integrated Dispatching System for Enterprise Railway[D]. Lanzhou Jiao tong University, 2013. (in Chinese)

[8] Hui P, Shi-Shan Z, Chang L, et al. Research on design of the object-oriented production scheduling rule base[J]. Manufacturing Automation, 2013. (in Chinese)

DOI: doi.org/10.26549/met.v3i1.1272

SYNERGY PUBLISHING PTE. LTD.

Modern Electronic Technology

https://ojs.s-p.sg/index.php/met

ARTICLE

Research on Distribution Network Automation and Distribution Network Planning Mode

Xuan Chen*

Changchun University of Technology, Changchun, Jilin, 130012, China

ARTICLE INFO

Article history
Received: 21 December 2018
Revised: 29 March 2019
Accepted: 8 April 2019
Published Online: 16 April 2019

Keywords:
Distribution network automation
Distribution network planning
Mode research

ABSTRACT

Based on the research of distribution network automation and distribution network planning mode, the analysis of the significance of urban distribution network automation must be performed at the first place. Combined with the problems existing in China's current distribution network, it is concluded that, establish effective hardware support system, data sharing and feeder automation to ensure automation safety; strengthen power distribution and power line material testing to improve distribution automation system and distribution network planning; research methods of improving the professional skills and comprehensive quality of professionals.

1. Introduction

The development of social economy has gradually improved people's living standards. To a certain extent, people have put forward higher requirements for their living environment and quality of life. The urban process is accelerating, and electricity consumption is constantly occurring. As an important energy source in people's living environment, electric energy is constantly increasing in demand for electric energy. Therefore, in order to ensure the quality of the use of electric energy, it should ensure that the grid can be effectively operated, and relevant personnel should do a good job in grid planning. However, in the process of actual work, it will be affected by many factors, which will further affect people's life and work. To improve the operation efficiency of the distribution network, it is necessary to apply the automation system in the urban distribution network environment and implement real-time monitoring of the distribution network application, so as to ensure the normal operation of the urban distribution network.

2. The Analysis of the Significance of Urban Distribution Network Automation

Power enterprises should ensure the stability of power supply and the quality of power distribution. Therefore, innovation and development of automation technology and computer technology are needed. The application of distribution network automation can save a lot of manpower and material resources and avoid cost waste. At the same time, it can also avoid the failure of power supply, improve the quality of urban power supply, and play an important role in the power supply system. Therefore, the application of distribution network automation systems plays an important role in power enterprises. The main

**Corresponding Author:*
Xuan Chen,
Changchun University of Technology, No. 2055 Yan'an Avenue, Changchun, Jilin, 130012, China;
E-mail:1205844669@qq.com

 DOI: https://doi.org/10.26549/met.v3i1.1325

role of urban distribution network automation is mainly for the main operation of the power system, and it is convenient to dispatch automation power. Distribution network automation technology is formed using a variety of technologies, which is a new science and technology, not only with remote operation, but also control of the power system, which guarantees the stable operation of the power system on a certain basis and effectively maximizes the economic benefits of the enterprise.

At present, in the process of urban distribution network operation in China, it is necessary to ensure the stability of power supply. Distribution line wiring can be affected by many factors, because the power supply line is affected by the external environment and will be affected for a long time. But now there are many power supply units that gradually bury the electrical lines underground. At present, there are many urban distribution network lines using cables, which improved the power supply effect to a certain extent, making the application of urban distribution network automation more convenient and promoting the rapid development of the city.[1]

3. Existing Problems in China's Distribution Network at the Present Stage

3.1 Problems with Power Supply Layout

At this stage, during the operation of the distribution network, there are generally some problems, and the power loss is relatively high. There are many areas in China that have established grid systems very early. Therefore, the actual distribution of the power point is not combined with the actual situation, and the distribution is unreasonable. However, the power supply radius is relatively long in some areas, and there is also a phenomenon of line damage. Such problems seriously lead to serious problems in the process of power transmission. In the process of power system operation, the quality of materials used is relatively poor, which will seriously affect the future development of power enterprises.

3.2 The Overall Structure Is Not Reasonable Enough

At present, there are many problems in the design of power grid structure in China, and to a certain extent, affect the supply of electricity, which will be limited by many factors, and people will be affected by electricity consumption in their daily lives.

3.3 Transportation Channel of the Distribution Network

In the process of urban distribution network planning, it is usually necessary to build cables and overhead lines, so as to keep up with the network operation of the distribution network. However, such construction costs are relatively high, and in the process of concrete construction, it will be affected by many factors.

3.4 The Degree of Distribution Network Automation Construction Is Relatively Backward

The construction of China's distribution network is relatively late. Therefore, in the process of construction, it is relatively low and cannot meet the development needs of social power. In fact, the scope of distribution network automation needs to be extensive. In the process of automation of distribution network, it often costs a lot of money. At present, in the process of building automation network for distribution network, China has certain requirements for equipment selection and technologies, and it needs to be strengthened in the management mode. These factors directly affect the normal operation of the entire distribution network system.

4. Research on the Methods of Urban Distribution Network Automation

At present, many countries use distribution network automation systems and have achieved certain results. However, relevant staff should also be aware that the actual situation is more complicated. At present, some regions have no strength and cost investment, and there are no corresponding problem-solving measures, which will hinder the future development of power enterprises to a certain extent. At the same time, there are still many problems in the power supply enterprises, such as mechanical equipment and management, which limits the development of urban distribution network automation technology. In this paper, the urban distribution network automation is studied from four aspects: distribution network frame equipment, Informatization system, automation system, and automation communication.

4.1 Establish an Effective Hardware Support System

Forecast the hardware in the market, collect the data in a scientific way, and combine the data for detailed analysis, which can accurately predict the demand for electricity, and there is a more powerful function that predicts the distribution of future electricity use. The use of electricity management repair system, power management is mainly through the network information system for management and supervision, if there is any abnormal situation of electricity, alarm, reduce safety is the occurrence of accidents,

DOI: https://doi.org/10.26549/met.v3i1.1325

which fundamentally guarantees the people's life safety and significantly improves the practical level of distribution automation engineering, making the distribution network automation system improve the reliability of power supply and effectively promoting the engineering quality and social and economic benefits.

4.2 Data Sharing

In fact, the automation technology of the power system has high requirements, effectively promoting the sharing of data within the system. In the process of data sharing, relevant departments of the enterprise should establish an independent management organization to strictly manage the power system. Analyze in the context of the entity, and define and improve the standardization, for the area covered by the power system, and also need to have data information of physical attributes, and then standard expression. The dependence of people's life on the power system, the distribution network has become an important part of life, so the government and relevant departments should pay attention to the power system. Therefore, it is necessary to analyze the actual situation, make overall plans for the operation of the system, adjust the parts locally, and effectively realize the automation of the power system, thereby improving economic benefits.

4.3 Feeder Automation

In the process of grid system operation, an effective control plan should be formulated, which is an advantage for on-site control, which mainly achieves the purpose through the functions of the recloser and the segmenter, and establishes a monitoring mode platform, and the information collected by the feeder terminal is transmitted back to the main station. If there is a fault, effective measures should be taken, mainly to collect information for judgment and analysis, and remote control. In combination with the actual situation, a detailed plan for power restoration can be made under the cooperation of intelligent switch and short circuit, which can cut off the faulty circuit accurately and timely, and effectively control the fault area.

4.4 Ensure Automation Safety

Power system automation technology should have certain flexibility to ensure the normal operation of the power system. The power system automation technology can effectively adjust the power, which can ensure the workload and work risk of the staff. Power enterprises should formulate relevant policies and timely maintenance of the power system, because automation technology is very important for data recording and updating, and can effectively reduce the cost budget in daily operations. But for the staff, the most basic thing is to ensure the safety of the employees. Power system automation technology has certain monitoring capabilities, and what abnormal problems occur in actual work, especially when a safety accident occurs, the automation system can promptly remind and take effective measures.

4.5 Strengthen the Detection of Power Distribution and Power Line Materials

In daily construction, leaders should pay attention to the detection of power transmission and distribution and power line materials. Before the work is carried out, the manufacturers of circuit materials should be selected. It is not necessary to purchase some materials that are not up to standard in order to reduce the cost of the enterprise. Therefore, strict inspection and testing are carried out before the safe operation of the transmission and distribution and power engineering lines, so that problems such as tripping during the use of the line can be effectively avoided. In the application of line materials in engineering, attention should be paid to the accuracy of line installation to ensure safe and reliable operation of the line.

4.6 Distribution Automation System

(1) In the process of urban distribution network automation construction, the adoption of information technology is a necessary condition. Building a complete distribution automation system requires unified integration and planning of distribution network data, user data and grid structure, and geographic graphics, which can effectively help monitor, protect and control the operation of the distribution network.

(2) At this stage, the urban distribution network automation system mainly uses GIS power distribution technology. In the process of computer integrated system operation, the geographic information system and production operation management technology are used for unified control of the distribution network planning. Specifically, it is the application of the GIS system, which can effectively maintain data parameters, network protocols, and the like. In the automatic generation of relevant data parameters, it should be combined with wiring diagrams, ring diagrams and one-line diagrams. But at the same time, when the power companies are using, they should strengthen production management, master the detailed information of customers, and comprehensively design the entire plan and plan, thereby improving the practicability of the system, effectively solving the problems of the data

 DOI: https://doi.org/10.26549/met.v3i1.1325

graph and improving the work efficiency.

(3) In the process of power system operation, to facilitate the access of data and communication interfaces, relevant staff should master the distribution of the structure and the application of the system, which will improve power quality and service to facilitate sharing data with other systems.

(4) The distribution network mainly monitors the remote area. The data acquisition and monitoring control system is mainly applied in the distribution network. At the same time, the terminal equipment and the communication system are accepted to understand the real-time status control. Among them, the real-time status usually refers to the data of the 10kV line column switch, ring network cabinet, distribution transformer and opening and closing station, protection action information and operation data.

(5) In order to ensure the expansion of the functions and scale of the distribution network automation system, the power system has the possibility of linear and seamless expansion. In the construction of distribution network automation system, adequate preparation should be made, mainly to determine the scale of the system, the size of the memory, the processing speed, etc., to effectively realize the realistic needs of the vision of distribution network automation.

4.7 Research on the Distribution Network Planning

In order to build a distribution network automation system quickly and efficiently, the distribution network planning should be done in advance. In the process of planning, the source of funds and system management should be considered comprehensively to ensure the normal operation of the distribution network automation system. In the process of construction, attention should be paid to the equipment itself and the problems of overweight and power supply capacity of the load. Moreover, in the work, the principle of ductility should be adhered to, and the current and substation should be comprehensively controlled. Relevant staff should make overall planning according to the actual development of local city distribution network automation, and must meet the actual requirements of automatic operation of distribution network. In the process of transforming the distribution network frame, distributed contribution should be carried out.

4.8 Improve the Professional Skills and Comprehensive Quality of Professionals

Power companies should pay attention to the training of dispatching staff. In the dispatching work, the professional skills and safety awareness of operators should be strengthened. Enterprises must implement safety management work. As a staff of power dispatching, they should be aware of the importance of power dispatching work, constantly absorb new working concepts in their work, and strictly abide by the relevant systems of power dispatching. In the actual work, the responsibility system for dispatching posts should be effectively implemented. The dispatching agency is an important department to ensure the safety, quality and economic operation of the power grid. With the development of society and the continuous improvement of people's living standards, society has a strong dependence on electricity, and the dispatching responsibilities of power grid workers are getting heavier and heavier. To this end, the grid dispatching system must have a high-quality cadre team and technical team.

5. Conclusion

In summary, in the continuous development of the social economy, we must strengthen the planning and design of the distribution network automation system. In this process, it is necessary to comprehensively analyze and comprehensively consider the automation system and characteristics of the distribution network in combination with actual needs and current conditions, under the support of modern science and technology, it can timely and effectively identify faults in distribution network operation, realize real-time control of distribution network operation, ensure the safe operation of distribution network, and promote the continuous development of China's electric power industry.

References

[1] Yu Du. Discussion on distribution network automation and distribution network planning mode[J]. Technology and Market, 2018, 25(09):148-149. (in Chinese) DOI:10.3969/j.issn.1006-8554.2018.09.069

DOI: https://doi.org/10.26549/met.v3i1.1325

SYNERGY PUBLISHING PTE. LTD.

Modern Electronic Technology

https://ojs.s-p.sg/index.php/met

REVIEW

Smart Classroom Design on the Basis of Internet of Things Technology

Lei Zhang*

Zhongkai University of Agriculture and Engineering, Guangzhou, Guangdong, 510225, China

ARTICLE INFO

Article history
Received: 16 November 2018
Revised: 29 March 2019
Accepted: 8 April 2019
Published Online: 16 April 2019

Keywords:
Internet of Things technology
Smart teaching base
Design
Realization

ABSTRACT

Internet of Things technology is a new type of network technology emerging in the new economic era. It has played a good role in various industries and provided new opportunities for the reform and optimization of the education industry. This paper takes the intelligent teaching base on the basis of Internet of Things technology as the research object, introduces the connotation of the wisdom teaching base with reference to relevant literature materials, analyzes the research background of the wisdom teaching base on the basis of the Internet of Things technology, expounds the design method of smart teaching base on the basis of Internet of Things technology, and analyzes the function realization and application of intelligent teaching base on the basis of Internet of Things technology.

1. Introduction

In the early 21st century, China's leaders regarded the Internet of Things as the key point of China's industrial development, providing a basis for the large-scale promotion and application of Internet of Things technology. The education and teaching platform on the basis of the Internet of Things technology is mainly through the design of the wireless communication module, and the original education and teaching base as the platform for the organic integration of product development and experimental teaching modules. Through the design and operation of the intelligent teaching base on the basis of the Internet of Things, the development efficiency of the overall education industry in China can be effectively improved. Therefore, it is very important to conduct an appropriate analysis of the intelligent teaching base on the basis of the Internet of Things technology.

2. Overview of the Smart Teaching Base

The Smart Teaching Base, also known as Smart Classroom, Future Classroom, etc., is an important component of the Smart Campus solution. The smart teaching base is an enhanced education and teaching base. It can realize the intelligent regulation and control of audio-visual equipment and seamless access of resources through the application of high-tech software and hardware equipment, which provides a basis for the improvement of overall classroom education and teaching management efficiency.

**Corresponding Author:*
Lei Zhang (1983),male, master degree, experimenter;
Correspondence address: Zhongkai University of Agriculture and Engineering, No. 388, Guangxin Road, Baiyun District, Guangzhou, Guangdong, 510225, China;
E-mail: zhanglei3563425@163.com.
Research direction: information security, food safety traceability, agricultural Internet of Things;

 DOI: https://doi.org/10.26549/met.v3i1.1221

3. Research Background of Smart Teaching Base on the Basis of Internet of Things Technology

Under the background of IBM's concept of smart earth, relevant professional scholars in China have further explored the construction of "smart teaching base" on the basis of Internet of Things technology. For example, Jian Yan, et al. proposed the overall design policy and layered design method of the campus Internet of Things infrastructure; Yonghua Zhou, et al. proposed the use of advanced information technology such as the Internet of Things to build a "smart teaching base" overall solution. [1,2] The above scholars' comments and elaboration of the "smart teaching base" research theory laid a solid theoretical foundation for the construction of smart teaching base on the basis Internet of Things technology.

4. Smart Teaching Base Design on the Basis of Internet of Things Technology

4.1 Principle of Smart Teaching Base on the Basis of Internet of Things Technology

The smart teaching base on the basis of the Internet of Things technology mainly uses the PLC controller as the terminal control module. Through the temperature, illumination detection, infrared detection, humidity data acquisition and wireless receiving signal acquisition, the internal data information of the teaching base can be obtained. Then, using the Internet of Things technology, the basic environment facilities such as lights and curtains in the teaching base can be automatically adjusted. Such as lighting energy control, automatic temperature and humidity adjustment, safety monitoring and warning, curtains opening and closing.

4.2 Physical Structure of Smart Teaching Base on the Basis of Internet of Things Technology

From the physical level of analysis, the smart teaching base on the basis of the Internet of Things technology mainly includes three modules: the sensing control layer, the information transmission layer, and the practical application layer. The sensing control layer can be further divided into an intelligent controller, a teaching base controller, and other types of sensors. The intelligent controller is the main channel for the transmission of the main control equipment and auxiliary equipment information of the whole teaching base; and the teaching base controller and intelligent sensor are the main basis for the self-control of the education and teaching base.

The smart teaching base transmission layer on the basis of the Internet of Things technology mainly uses the wireless LAN as a channel to interact with the application layer servers for effective data information.[3]

The smart teaching base application layer on the basis of the Internet of Things technology mainly realizes real-time sharing of data information of each teaching base controller by using the wireless LAN technology in each teaching base by setting the smart teaching base server.

4.3 Design Goals of Smart Teaching Base on the Basis of Internet of Things Technology

The smart teaching base is designed to transform the education and teaching base into a comprehensive self-control system on the basis of the use of Internet of Things technology and intelligent equipment under the premise of multimedia classrooms and professional training classrooms. Firstly, in the design process of the conventional hardware setting, it should be ensured that the smart teaching base has an electronic whiteboard, a short-focus projector, a physical exhibition stand, a wireless microphone, a smart processor, a high-definition digital television, an audio device, an electronic school bag and the like.

Secondly, in the process of setting up the internal environment of the teaching base, the internal temperature of the teaching base should be controlled by the Internet of Things sensing technology to be around 22.0-25.0 °C; while in the teaching base, the lighting and power lighting design module can use the FRID technology to set the intelligent adjustment of light intensity. .

Finally, in the teaching internal teaching resource transmission module, the smart teaching base on the basis of the Internet of Things technology should have the FRID embedding device inside, so that the PC teaching information of the course teaching staff can be automatically transmitted and displayed.

4.4 Design of Smart Teaching Base on the Basis of Internet of Things Technology

Firstly, the human body position detection mode is set. The human body position detection is the main component module of the smart teaching base intelligent sensing device. It can timely adjust the lighting, electric fan and other devices through the analysis of the distribution information of the personnel inside the teaching base. Considering the construction cost and control efficiency of smart teaching base, in the process of setting the human body position detection mode of the smart teaching base on the basis of the Internet of Things technology, the sin-

DOI: https://doi.org/10.26549/met.v3i1.1221

gle bus mode can be adopted to divide the overall human body position detection mode into a detection module and a main control module, and the two are in the form of a single bus serial networking. The main control module mainly includes a single bus interface unit, an infrared detection unit, a ZigBee wireless transmission unit, a main control unit MCU and the like; the detection module mainly comprises two modules: an infrared detection unit and a single bus interface unit.

In the actual operation process, the main control unit MCU can collect the infrared detection unit operation data through the single bus interface unit. And through the ZigBee wireless transmission unit and the internal functional equipment of the teaching base for information exchange. During the operation of the main control unit, the infrared detection unit could timely sense the number of people gathered in each area of the smart teaching area; and the single bus interface unit can build an efficient information interaction channel between the main control module and the detection module.

Secondly, in the lighting control module, Chinese scholars have done a lot of research and development. For example, the design of Lang Zhou, et al. has realized a device on the basis of the Internet of Things technology to accurately identify the movement and static characters in the teaching base to control the on/off of the lights, and effectively realize the intelligent control of the internal lighting of the teaching base.[4] According to the changes in the internal use of the teaching base, the internal lighting control methods of the teaching base have also changed. Therefore, in the process of setting up the lighting control module of the teaching base, the multi-level stereo teaching base lighting control model can be constructed by combining the human body detection sensor distribution mode to realize the intelligent remote control of the internal lighting of the teaching base. The teaching base will be divided into several modes: examination, self-study, idle, and class. Using the policy control mechanism, the overall control strategy is set to: control strategy = ({teaching base, time period, use, control method, week})

The teaching base control method is mainly: control mode = (automatic control / semi-automatic control / full open / full closure)

In the "automatic control" mode, the internal lighting device of the teaching base will automatically adjust according to the illumination level of the teaching base and the location of the crowd; In the "semi-automatic control" mode, the teaching base lighting device can open the manual intervention channel in the terminal control module button unit on the basis of the terminal control, so that the distribution base of the teaching base can be reasonably adjusted according to its own needs; In the "full open" mode and the "full closure" mode, the internal lighting devices of the teaching base are located in the manual control module, and the terminal automatic control module cannot intervene. That is, the user can manually define the lighting control according to changes in the internal use of the teaching base. For example, for a long-term idle teaching base, it can be set to a "full closure" state.

5. Realization of Smart Teaching Base on the Basis of Internet of Things Technology

5.1 Composition of Smart Teaching Base on the Basis of Internet of Things Technology

Smart teaching base on the basis of Internet of Things technology mainly includes lighting distribution and remote alarm indication, control panel and sensor display, module display and other aspects. The lighting distribution and remote warning indications of the teaching base mainly include different types of indicator lights, such as light warning instructions; The control panel and sensor display mainly include several modules such as photosensitive sensor, nine-key panel, wind control panel, infrared sensor, multi-function touch screen, temperature and humidity sensor; The module display mainly includes several modules such as AC touch device, relay and PLC control device. The above modules can be connected to different types and color wires to realize the full circuit control of smart teaching base.[5]

5.2 Function Setting of Smart Teaching Base on the Basis of Internet of Things Technology

The smart teaching base function module on the basis of Internet of Things technology mainly includes networking functions, security anti-theft and remote warning of teaching base, automatic distribution and control of teaching base lighting, environmental monitoring and self-adjustment of teaching base. The networking function module mainly uses the network communication port in the terminal PLC controller to perform reasonable setting of the controller and the computer server in the same network segment of the same router. Combined with the mobile smart terminal touch screen application, effective network transmission is realized. During the operation of smart teaching base, the teaching staff can use the mobile intelligent terminal or computer server to control all network interfaces to ensure the smooth progress of classroom teaching.

The security base and remote warning of the teaching

 DOI: https://doi.org/10.26549/met.v3i1.1221

base are mainly through the reasonable setting of the door closing and arming function. If there is no light in the teaching base area or the door and window are opened without any reason, the remote control can be closed by computer software. If there is an illegal intrusion in a time other than classroom teaching, the computer terminal server and the intelligent terminal will also have an alarm message, so that the staff at the teaching base can be informed in time.

In the operation process of the education and teaching base on the basis of the Internet of Things technology, the terminal control module can perform independent power control on all lighting devices in the teaching base according to a preset program. And automatically open and close according to the standard of work and rest. At the same time, according to the internal illumination of the teaching base, the curriculum, the work schedule and the number of people, the system terminal control module can also monitor the running status of each lighting device in real time, and transmit the relevant information to the intelligent control terminal via the internal network of the teaching base, so as to ensure sufficient lighting supply and lighting energy management effects. In the teaching base lighting self-distribution and control module, according to the scope of education and teaching base and the number of people, different control modules can be used. For an education and teaching base with a large scope and a large number of people, the number of people can be controlled by sub-regional control. For an education and teaching base with a small distribution area and a small number of people, a static human body induction centralized control method can be adopted. Through the application of different control methods, during the normal operation of the teaching base, the system terminal control module can effectively determine the lighting information of each module and reasonably adjust the internal light intensity and strong illumination area of the teaching base.

The environmental monitoring and self-regulation of the teaching base mainly consists of setting different types of sensing elements inside the teaching base, such as temperature and humidity sensor elements, infrared sensing elements, carbon dioxide gas sensing elements, smoke sensing elements, and the like. By monitoring the internal illumination, carbon dioxide concentration and temperature and humidity of the teaching base in real time, the bad air condition inside the teaching base can be sensed in time, and the prevention and control adjustment is automatically carried out.[6] If the internal light intensity is higher than the standard value in the teaching base, the terminal control module will automatically execute the electric curtain closing procedure; when the carbon dioxide concentration in the teaching base is higher than the standard design value, the terminal control module will automatically execute the ventilation opening procedure to ensure that the teaching base teaching work goes smoothly.

6. Software and Hardware Settings of Smart Teaching Base on the Basis of Internet of Things Technology

Firstly, in the process of setting the structure of the human body position detecting unit, the overall teaching base can be divided into corresponding number of detecting sub-modules according to the existing application situation of the teaching base. A reasonable setting of the detection module or the main control module is then carried out in the ceiling area above the corresponding detection sub-module. At the same time, the detection module and the main control module are connected in a single bus serial connection manner. Through the single-bus periodic polling, combined with the detection module networked operation, the application running information of the teaching base can be fed back in real time.

Secondly, in the process of setting the software parameters of the actual teaching base, it can be reasonably adjusted according to the changes of specific operational requirements. For example, in the "Reminder Service" setting process, on the basis of the curriculum information, 30min or 60min can be set in advance to provide the course start time and teaching location for the course teaching staff or learners.[7]

7. Application Effect of Smart Teaching Base on the Basis of Internet of Things Technology

According to the previous design requirements, a teaching base uses TI CC2531, stm32F108, CC2531 to design and implement all intelligent sensors, intelligent control devices and intelligent applications, and realizes effective control of various smart teaching base application modules, which provides a good basis for the improvement of the operational efficiency of the teaching base. Course faculty members can directly use the IC card to conduct remote operation of the equipment at the beginning of the prescribed course, effectively avoiding the frequent influence of the property manager on the efficiency of the multimedia course.[8] At the same time, using the campus card, the course learners can also automatically punch the card, providing a basis for the course management personnel to know the learning situation of the course learners in time; In the self-study course, the course learners can automatically query the existing number of self-study

DOI: https://doi.org/10.26549/met.v3i1.1221

teaching bases and self-study teaching bases with the help of the smart guidance service, and improve the resource utilization efficiency of the self-study teaching base; In the process of routine teaching management, through the application of Internet of Things technology, environmental information can be detected on the basis of sensors. Combined with the operation of air conditioners, fans, curtains and lighting devices, the established control scheme is set up, which effectively improves the utilization efficiency of equipment resources within the teaching base.

8. Conclusion

In summary, the classroom education teaching work is an important component of the education industry, and in the process of modern technology development, the past education and teaching base can no longer meet the needs of contemporary education and teaching. Therefore, in the process of comprehensive reform and optimization of the education and teaching industry, educational institutions should increase the application of new technologies such as Internet of Things technology, and organically integrate intelligent teaching and intelligent control of teaching bases. Through the reasonable setting of environmental monitoring self-regulation, lighting self-distribution control, remote warning and other functional modules, thus providing guarantee for the smooth development of classroom education and teaching work.

References

[1] Jian Yan, Jinsong Gui. Design and Realization of Smart Teaching Base Based on Internet of Things Technology[J]. China Electro-chemical Education, 2016 (12):83-86. (in Chinese)

[2] Yonghua Zhou. Design and Realization of Smart Teaching Base System Based on Internet of Things[J]. Electronic Technology and Software Engineering, 2018(9): 256-257. (in Chinese)

[3] Jun Liu. Design of Smart Teaching Base in Colleges and Universities Based on Internet of Things Technology[J]. Journal of Shaanxi University of Technology (Natural Science Edition), 2017, 33(5):52-57. (in Chinese)

[4] Lang Zhou, Zhe Lin, Xiaofang Hu, et al. Design and Realization of a Smart Teaching Base Based on Internet of Things[J]. Wireless Communication Technology, 2014, 23(4): 53-56. (in Chinese)

[5] Pengyi Zhang, Zhaojun Liu. Design of Smart Teaching Base IoT Teaching Platform Based on PLC Control[J]. Shandong Industrial Technology, 2017(17):76-76. (in Chinese)

[6] Shunyong Zhao. Design and Research of Smart Teaching Base Based on Internet of Things[J]. Journal of Fujian Computer, 2017, 33(2):124-126. (in Chinese)

[7] Huanzhi Qiu, Yongcan Chen, Chaosheng Fan, et al. Analysis of Smart Teaching Base System Based on WiFi Internet of Things Technology[J]. Enterprise Technology Development, 2016, 35(3):62-63. (in Chinese)

[8] Enhao Zhou. Design and Realization of Smart Teaching Base Internet of Things System in Colleges and Universities[J]. Modern Electronic Technology, 2018, 41(2):30-33. (in Chinese)

 DOI: https://doi.org/10.26549/met.v3i1.1221

SYNERGY PUBLISHING PTE. LTD.

Modern Electronic Technology

https://ojs.s-p.sg/index.php/met

REVIEW

Automatic Measurement and Control Design of Sea Wave Energy Storage and Seawater Desalination Device

Zhihao Dou[1], Yimeng Luo[2], Chunye Li[3*]

1. Southwest University, Chongqing, 400715, China
2. Xidian University, Xi'an, Shaanxi, 710126, China
3. State Grid Shanxi Electric Power Company, Taiyuan, Shanxi, 030001, China

ARTICLE INFO

Article history
Received: 29 March 2019
Revised: 4 April 2019
Accepted: 8 April 2019
Published Online: 16 April 2019

Keywords:
Sea wave energy storage
Seawater desalination
Automation

ABSTRACT

The application of seawater desalination has become more and more popular. The reverse osmosis membrane method is one of its applications, but it consumes more energy resources and produces freshwater with high cost. The four-column floating bed we designed has low investment and is simple and easy to operate. The sea wave energy storage and seawater desalination device produced by this method has greatly reduced the cost of freshwater produced. This paper focuses on the design of the automatic measurement and control loop of the device.

1. Introduction

There are many places where the sea is lacking freshwater, making the seawater desalination become popular. At present, various seawater desalination methods consume a lot of energy, resulting in high crude water costs. Some units have experimented with the use of wind power from the sea and the power generated by solar energy to drive seawater desalination, so that the sea can send freshwater to shore. It seems feasible, but the current investment in wind and solar power is too large, and the cost of converted freshwater is too high, which is difficult to promote.

At present, the most widely used method for seawater desalination is the reverse osmosis membrane method.[1] The factors that hinder its widespread promotion are also too much energy consumption and high freshwater cost.

2. The Implementation Scheme of Sea Wave Energy Storage and Seawater Desalination Device

We invented the "sea wave energy storage and seawater desalination device", which is located in the shallow beach, does not consume additional energy, and can operate by collecting the waves, so that the sea can send fresh water to shore. At the same time, the total investment is very low, the cost of converting fresh water is very low, and it has a good promotion prospect. This invention has been applied for China's utility model technology inven-

**Corresponding Author:*
Chunye Li,
State Grid Shanxi Electric Power Company, No. 71 Fudong Street, Taiyuan, Shanxi, 030001, China;
E-mail: k36958@sina.com.

DOI: https://doi.org/10.26549/met.v3i1.1538

tion patent. Methods as below:

(1) A four-column floating bed is designed: a rectangular bed is made of corrosion-resistant angle steel, and a foam block is bound under the bed body, so that the bed body and the equipment thereon float on the water surface; On the beach, four columns are arranged. The outside of the column is covered with a cylinder about 40 cm long. The cylinder is spaced about 0.5 cm from the cylinder. The cylinder is linked with the four corners of the floating bed. In this way, the floating bed floats with the tide level, but it is not shaken by the impact of the waves. All equipment is installed on a floating bed.

(2) A floating grille is mounted on the side of the floating bed, and the duck head floating body is installed in the grille. The movement of the waves promotes the movement of the duck-headed floating body, and the plunger pump is moved by the lever to pressurize the seawater or fresh water. This is the driving force for the operation of the device. After testing, the wind force is about three levels, and each plunger pump has an output of about o ton of water per hour. The seawater is filtered by the secondary filter before being pressurized by the medium-pressure pump and the drug is detoxified and descaled, and then pressurized by the high-pressure pump. After being pressurized, the seawater is sent to the stabilized water storage tank through the check gate.

(3) After the water storage tank, the seawater is sent to the reverse osmosis membrane filter cartridge through the control valve. The membrane used in the reverse osmosis unit is a composite membrane suitable for seawater.[2] The SWHR-380 seawater membrane produced by American Dow Company has a desalination rate of 99.6% for a single filter cartridge. The desalinated water from the filter cartridge enters the manifold. After the filter cartridge is concentrated, the seawater is discharged through the control valve. The fresh water of the manifold is then pumped to the land via a plunger pump. In this way, only the seawater energy is used to desalinate the seawater and send it to the land, and the equipment cost is low, and the cost of fresh water can also be low.

The schematic diagram of sea wave energy storage and seawater desalination device is as follows (Figure 1).

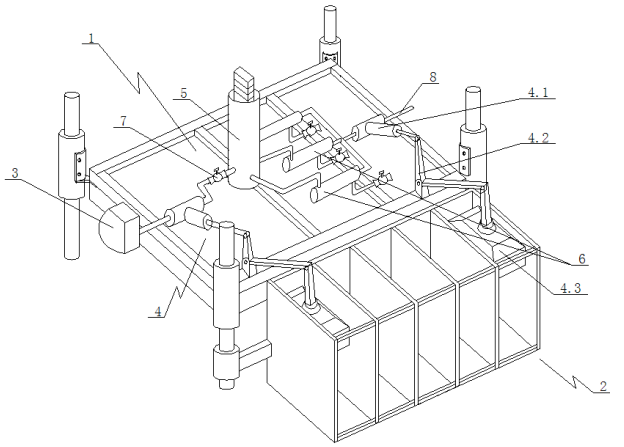

Notes: 1. Floating bed; 2. Grille; 3. Filter; 4. Plunger pump; 4.1 Freshwater booster pump; 4.2 Transmission rod; 4.3 Duck head float; 5. Regulated water tank; 6. Reverse osmosis cartridge; 7. Check valve; 8. Fresh water outlet pipe

Figure 1. The schematic diagram of sea wave energy storage and seawater desalination device

3. The Design of Device's Measurement and Control System

Compared with conventional terrestrial desalination devices, the difference is that the power is derived from wave energy rather than electricity; the whole set is installed in sea water instead of on land. It is impossible for someone to control it on site. There must be a practical, simple and reliable remote measurement control system.[3] Due to the filtration, dosing, pressurization, desalination and other processes of seawater, it is similar to the conventional reverse osmosis seawater desalination process, and there is no operation of equipment such as motors. The monitoring and control is relatively simple. The output of the whole device, that is, the output of the finished fresh water is determined by the size of the wave energy at that time, that is, "depending on the weather". We have a monitoring room on the land, and there are process simulations of all the equipment on the panel, showing the operating status of all the equipment. Just set up remote control switches for several key devices.

(1) Measurement and control of pretreatment system: We adopted the automated measurement and control system based on PLC and human machine interface (HMI) designed by Tianjin Seawater Desalination Research Institute. Measurement and control of the inlet screen: Due to the convenience of direct access to the beach, the fence area is large. A three-stage filter screen is provided. The first-stage filter fence has a volume of 100 cubic meters, and intercepts objects of more than 3 centimeters. The second-stage filter fence has a volume of 10 cubic meters,

 DOI: https://doi.org/10.26549/met.v3i1.1538

intercepts objects of more than 1 mm, and adds flocculating agents and descaling agents. The third-stage filter is a 5 micron security filter, which is equipped with a cone filter rod made of polypropylene spray, deep filtration, and large amount of dirt, long life and easy replacement. The third stage is provided with two sets of filter screens. The PLC collects the pressure on the two sides of the filter screen, switches the filter screen according to the pressure difference on both sides, and automatically backwashes.

(2) Since the operation of the plunger pump is unstable and the outlet pressure is unstable, the plunger pump outlet is added with a check valve. The opening and closing monitoring point of the back door can display the running condition of the plunger pump.

(3) The pressure inside the regulated water storage tank is adjusted by the number of top weights. A position monitoring point is installed every 5 cm in the water level in the tank.

(4) There are 5 reverse osmosis membrane cartridges, and each filter cartridge inlet valve is electrically controlled. When the water level in the water storage tank is the highest, the entire filter cartridges are opened, and a filter cartridge is stopped for every 5 cm of the water level. The PIC monitors the transmembrane pressure difference in real time. When the transmembrane pressure difference increases by 10%, it exits the work for cleaning. In order to extend the working cycle of the filter cartridge and reduce the number of cleanings, according to the characteristics of the device, the concentration ratio of seawater is reduced. After the filter cartridge is concentrated, the seawater is discharged through the electric control valve. The desalinated water from the filter cartridge enters the manifold.

(5) The fresh water in the manifold is then sent to the land by a plunger pump.

(6) Solar power panels and small wind turbines and accumulators are installed on the four columns to provide power for the measurement and control device.

(7) There are two safety measures for avoiding wind and waves: first, the predictable wind and waves, untie the link between the floating bed and the cylinder on the column, and drag the floating bed to the safe area; second, suddenly encounter the wind is greater than five levels, start the safety protection device, temporarily loosen some of the foam blocks bound to the floating bed, so that the floating bed sinks to avoid danger.

(8) The monitoring point signals of the device are transmitted to the monitoring room via the optical cable.

4. Conclusion

The four-column floating bed described in this paper provides an ideal platform for the collection and utilization of wave energy. Based on this, sea wave energy storage and seawater desalination device was designed, which realizes the human ideal that the ocean itself sends fresh water to the land and the cost is low, which is worth promoting. This paper focuses on the automatic measurement and control part of the device.

References

[1] Kening Wang, Jinyan Wang. Design and Application of Automatic Monitoring System for Reverse Osmosis Seawater Desalination[J].Water & Wastewater Engineering, 2016, 42(3):134-136. (in Chinese)

[2] Chao Li, Liping Li. Application of automation technology in reverse osmosis seawater desalination system[J].Manufacturing Automation, 2014, 0(14):87-90. (in Chinese)

[3] The “sea wave electric generator” independently developed by Chinese scientists has obtained multinational patents[EB/OL]. China Machine Net, http:www.jx.cn. (in Chinese)

DOI: https://doi.org/10.26549/met.v3i1.1538

SYNERGY PUBLISHING PTE. LTD.

Modern Electronic Technology

https://ojs.s-p.sg/index.php/met

REVIEW

An Optimization Algorithm of Circular Interpolation Aiming at Point-by-Point Comparison Method

Xiaochun Shu[1*], Xiaoling Huang[1], Qianbao Cheng[2], Yan Li[1], Liyong Hu[1]

1. Xuancheng Vocational and Technical College, Xuancheng, Anhui, 242000, China
2. Xuancheng Municipal Sunbu Town Central Junior High School, Xuancheng, Anhui, 242000, China

ARTICLE INFO

Article history
Received: 1 April 2019
Revised: 4 April 2019
Accepted: 8 April 2019
Published Online: 16 April 2019

Keywords:
Interpolation
Circular interpolation
Pulse equivalent

ABSTRACT

Interpolation technology is the core technology of numerical control technology, and the requirements for curve processing in numerical control machine tools are getting higher and higher. According to the current development of numerical control machining, the optimization of the interpolation technology for arcs is proposed,[1] and the improvement is proposed in the original feeding mode which not only improves the calculation speed of the interpolation, but also improves the processing efficiency. In addition, the improved algorithm can reduce the machining error so that the error can be reduced to within the range of 0.5 pulses equivalent.

1. Introduction

At present, computer technology is developing rapidly. Some complicated surface parts can be easily realized by software. The numerical control machine cannot easily realize complicated curve or track processing, most machines use a small straight line segment to force the contour. The smaller the length of the line segment, the closer the feeding path of the tool is to the contour of the part, but it also generates a lot of data. Under normal conditions, the machining accuracy of the machine tool is doubled, and the amount of data generated is several times the accuracy. Conversely, in order to reduce the amount of data, of course, it will facilitate transfer and storage, which will result in reduced processing contour accuracy.[2,3] In response to the above problems, some numerical control systems want to obtain a stable feed rate and perform pre-processing. However, on the common economical numerical control machine, the point-by-point comparison algorithm is used to approximate the line, which may result in a pulse error. An improved scheme for the point-by-point comparison algorithm can reduce the error to within 0.5 pulses,[4] so it is also called the half-step deviation method.

2. The Basic Principle of Half-step Deviation Method

The half-step deviation method is optimized for the feed-by-point comparison method. The point-by-point

**Corresponding Author:*
Xiaochun Shu, Xuancheng Vocational and Technical College, No. 698 Xunhua Road, Xuancheng, Anhui, 242000, China;
E-mail: 25809453@qq.com.

Fund Project:
The Scientific Research Revitalization Plan of Xuancheng Vocational and Technical College (Cultivation Plan——Analysis and Research of the Interpolation Algorithm of Numerical Control Stone Carving Machines) (Project No.: ZXPY201812).

 DOI: https://doi.org/10.26549/met.v3i1.1603

comparison method divides the plane coordinate system into 4 quadrants and moves to the X-axis or Y-axis in the quadrant.[5] As shown in Figure 1 below, the current interpolation point is point P. According to the point-by-point comparison method, the next step is to feed the Y-axis to the point E. The minimum value of this point and the line is L_3. If the X-axis and the Y-axis are fed one step at a time, the point C is reached, and the minimum value of the point C and the straight line is L_2, $L_2 < L_3$; if the current X-axis and Y-axis are set to feed simultaneously (also called diagonal feed), a smaller deviation will be obtained,[6,7] the distance between BC in the figure is 1 pulse, BD + CD = 1, in addition, BD > L_1, CD > L_2; if BD ≥ 0.5, it is known that CD ≤ 0.5, because CD > L_2, it is known that $L_2 < 0.5$; if the next interpolation is performed from the current interpolation point P to reach point C, the error is controlled within the range of 0.5 pulses.

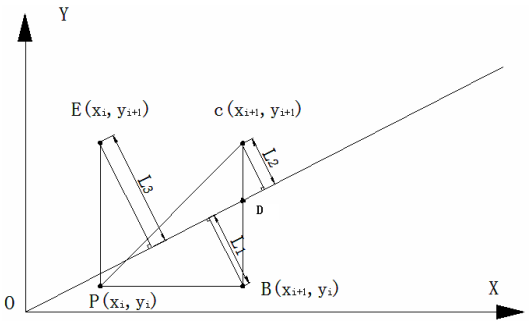

Figure 1. Feeding comparison of interpolation points

3. The Definition of the Deviation Value in Half-step Deviation Method

According to the above inferences, the plane is divided into 8 regions without considering the direction, and used to compare the coordinates of the interpolation end point coordinates, as shown in Figure 2 below.

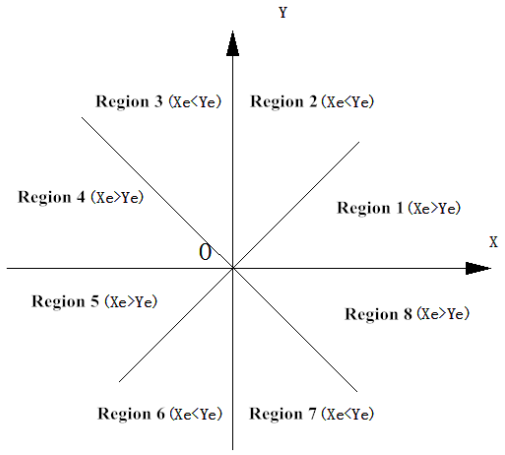

Figure 2. Division of linear interpolation regions by half-step deviation method

The regulations are as shown in Table 1 below:

Table 1

Serial Number	Conditions	The Direction of Feed
1	$X_e \geq Y_e$	Feed towards the one with smaller deviation between the diagonal direction and the X direction.
2	$X_e < Y_e$	Feed towards the one with smaller deviation between the diagonal direction and the Y direction.

The half-step deviation method calculates the one with the smaller deviation between *X/Y* and the diagonal direction before feeding. As the feed direction, for example, there is a point $P(X_i, Y_i)$, and the deviation is calculated as follows:

$$F_{ii} = X_e Y_i - X_i Y_e \tag{1}$$

(X_e, Y_e) is the value of the endpoint coordinate.

Starting at point P, if take a step towards X, the new deviation is:

$$F_{i+1,i} = X_e Y_i - (X_i + 1) Y_e \tag{2}$$

If take a step towards Y, the new deviation is:

$$F_{i,i+1} = X_e (Y_i + 1) - X_i Y_e \tag{3}$$

If take a step towards X/Y, the new deviation is:

$$F_{i+1,i+1} = X_e (Y_i + 1) - (X_i + 1) Y_e \tag{4}$$

For the sake of explanation, here is an example of straight line analysis.

Figure 3 is a schematic diagram of the half-step deviation feed. If there is a straight line starting from the starting point, the end point is (X_e, Y_e), and the straight line equation $y=kx(0 < k < 1)$ is in the Region 1. Since $X_e > Y_e$, the feed mode is ($\triangle x$) or ($\triangle x$, $\triangle y$).

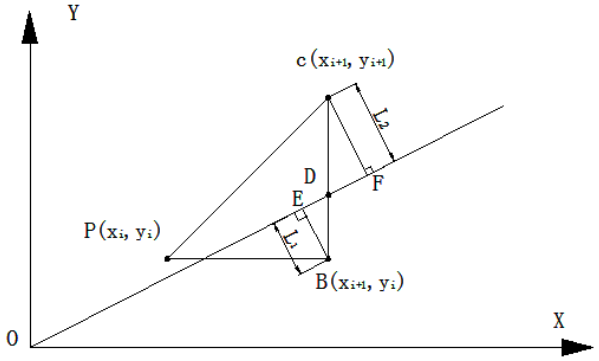

Figure 3. Schematic diagram of the half-step deviation method

The current point is $P(X_i, Y_i)$, then there are two pos-

DOI: https://doi.org/10.26549/met.v3i1.1603

sibilities for the next move. One is to go one step to the *X*-axis, to reach *B* (X_{i+1}, Y_i), and the other is to take the *X*-axis and *Y*-axis one step at the same time and reach *C* (X_{i+1}, Y_{i+1}). According to the first scheme, the distance between the position of the arrival point after interpolation and the straight line is L_1. If the interpolation is performed according to the second scheme, the distance between the position of the point reached after the difference compensation and the straight line is L_2.

As can be seen from Figure 3 above, △ *BED* is similar to △ *CFD*.

$BE/CF=BD/CD$

If $BD > Y$, it can be obtained that $L_1 > L_2$, and vice versa. The point at which is located after the interpolation is related to the linear distance and the deviation function. Figure 3 is simplified below to obtain Figure 4.

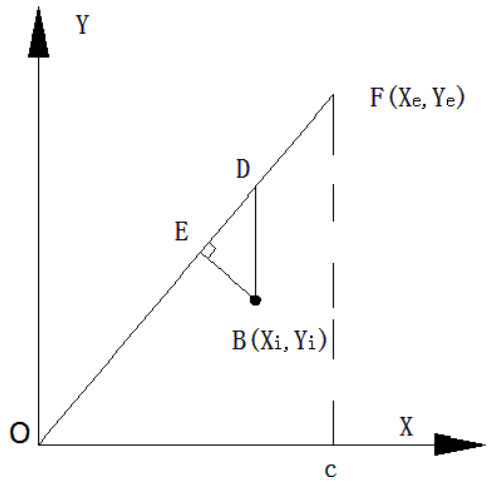

Figure 4. The deviation of the machining points

According to the value of F_{ii}, the distance between point *B* (X_i, Y_i) and the straight line is obtained, as shown in Figure 4:

△ *OFC* ∽ △ BDE, $BE/OC=BD/OF$, and then, it is known that $BE = BD/OF \times OC$. Let △ *L* be the shortest distance from point *B* to the line, the deviation of *B* (X_i, Y_i) is:

$$\begin{aligned} F_b &= X_e Y_i - X_i Y_e \\ &= X_e[(Y_i + BD) - BD] - X_i Y_e \\ &= X_e Y_D - X_N Y_E - X_e BD \\ &= -X_e BD \\ &= -OC \times BD \end{aligned}$$

$$\therefore \triangle L = |F_B/OF| = |F_B|/OF \quad (5)$$

Where $F_B = F_{ii}$

The deviation value of the △ *L* machining point *B* from the target straight line is referred to as the deviation.

It can be concluded that, Interpolated from the current point to the next target point (see *B*, *C* in Figure 3), The distance between the two target points (*B, C*) to the straight line (*BE, CF*) and the *BC* are linearly divided into two parts (*BD, CD*) in a proportional relationship ($CF/BE = CD/BD$). (That is to say, in addition to directly comparing the size of $|BE|$ and $|CF|$, the size of $|BD|$ and $|CD|$ can also be compared.)

From the definition of the half-step deviation method, if the interpolation algorithm of the half-step deviation method needs to compare the size of the distance line after the two feeds in the first region, the selection distance is small as the direction. In combination with the above analysis, the following equations (3) and (4) are compared, and the deviation function $|F_{ii} - Y_e|$ after one pulse is emitted in the X-axis direction is compared with the deviation function $|F_{ii} + X_e - Y_e|$ after one pulse is simultaneously emitted to the *X*-axis and *Y*-axis.

Set: $f = |F_{ii} + X_e - Y_e| - |F_{ii} - Y_e|$

If $f > 0$, the pulse is simultaneously sent to the *X*-axis and *Y*-axis;

If $f \leq 0$, the pulse is sent to the *X*-axis direction.

3.1 Mathematical Analysis of Half-step Deviation Method

3.1.1 The Circular Feed Rules of Half-step Deviation Method

The interpolation of the arc is more complicated, not only the quadrant problem of the starting point and the end point of the arc, but also the difference between the clockwise arc and the counterclockwise arc. The half-step deviation method circular interpolation is also evolved on the basis of point-by-point comparison method. As shown in Figure 5, the current interpolation point is P. According to the theory of point-by-point comparison method, it can be known:

$$R^2 = X_i^2 + Y_i^2$$

If the point P falls on the arc, the following formula holds:

$$X_i^2 + Y_i^2 = R^2$$

If the point P falls outside the arc, the following formula holds:

$$X_i^2 + Y_i^2 > R^2$$

If the point P falls inside the arc, the following formula holds:

$$X_i^2 + Y_i^2 < R^2$$

 DOI: https://doi.org/10.26549/met.v3i1.1603

In the point-by-point comparison method, let $X_i^2 + Y_i^2 - R^2$ be the deviation discriminant F_{ii}.

When $F_{ii} \geq 0$, the machining point falls on the arc or outside the arc, and one pulse equivalent is fed to -*X* at this time;

When $F_{ii} < 0$, the machining point falls within the arc and a pulse equivalent is fed to +*Y*. Based on the point-by-point comparison method, the following inferences are made:

Let point *P* be in the first quadrant and the central angle is less than 45°, point *P* is outside the arc. The next step is to feed the -*X* direction and reach point *C*. If let it move (-X, Y) two axes at the same time, reach point *B*. Let point P coordinate be interpolation coordinate *P* (X_i, Y_i), point *B* coordinate be *B* (X_{i-1}, Y_{i+1}), point *C* coordinate be *C* (X_{i-1}, Y_i), *CD* + *BD* =1, *B*, and the distance between *B* and *C* is 1 pulse equivalent. As can be seen from the figure, the distance from point *C* to arc is L_1, and the distance from point *B* to arc is L_2. The half-step deviation circular interpolation is similar to the half-step deviation linear interpolation. It is necessary to compare the sizes of L_1 and L_2 and select the direction with small deviation.

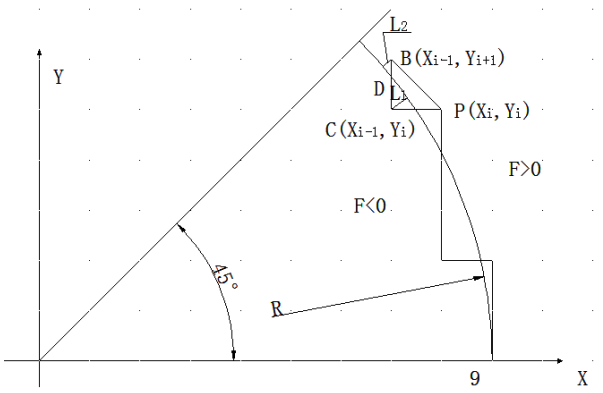

Figure 5. The counterclockwise arc in the first quadrant

According to the point-by-point comparison method region division rule, the half-step deviation circular interpolation divides the plane rectangular coordinate into 8 regions, and the feeding of each region is as shown in Figure 6. In the figure, the big circle is a counterclockwise circular interpolation of the feed route of each region, and the small circle is a clockwise circular interpolation route.

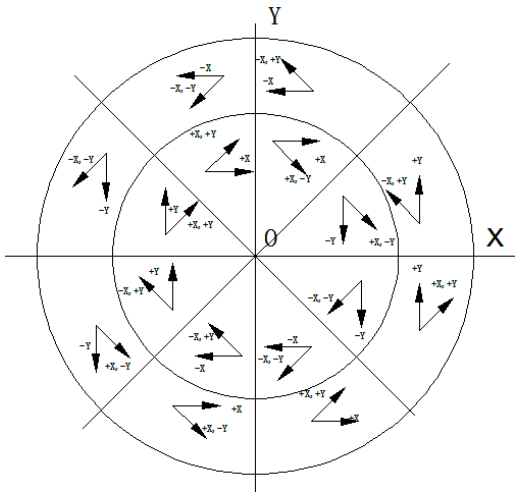

Figure 6. The coordinate feed directions of clockwise and counterclockwise arcs in plane coordinate system

In order to ensure the error of half-step deviation method, the direction of feed is determined according to the following principles:

(1) When $X \geq Y$, one pulse is taken in the positive direction of *Y*, or one step is taken in the positive direction of -*X* and +*Y*.

(2) When $X < Y$, one pulse is taken in the positive direction of *X*, or one step is taken in the negative direction of -*X* and +*Y*.

3.2 The Feed Discriminant of Half-Step Deviation Method

3.2.1 Point-By-Point Comparison Method Interpolation Feed Discriminant and Calculation Formula

In the whole point-by-point comparison method, the addition and subtraction operations and multiplication operations are needed, which directly affects the entire operation speed, if the whole hardware device is added for the dedicated control machine, most of them use its simplified algorithm, called iterative method, and some are called recursive method.

(1) If the first quadrant map is taken as an example, if the deviation value $F_{ii} \geq 0$, one pulse is sent to the positive direction of the X-axis, and the tool is fed one step forward from the current point (X_i,Y_i) to the X-axis to reach the new point (X_{i+1},Y_i), $X_{i+1}= X_i+1$, Thus, the deviation function value of the new machining point is:

$$\begin{aligned} F_{i+1,i} &= X_e Y_i - X_{i+1} Y_e \\ &= X_e Y_i - (X_i + 1) Y_e \\ &= F_{ii} - Y_e \end{aligned} \tag{6}$$

DOI: https://doi.org/10.26549/met.v3i1.1603

If the deviation function $F_{ii} < 0$, one feed pulse is sent to the positive direction of the Y-axis, and the tool feeds one step from the current machining point (X_i, Y_i) to the Y direction to reach the point (X_i, Y_{i+1}), where $Y_{i+1} = Y_i + 1$, the deviation function value of the point is

$$\begin{aligned} F_{i,i+1} &= X_e\left(Y_i + 1\right) - X_i Y_e \\ &= F_{ii} + X_e \end{aligned} \tag{7}$$

3.2.2 Half-step Deviation Method Interpolation Feed Discriminant and Calculation Formula

According to the principle of point-by-point comparison method, in order to reduce the influence of the algorithm on the operation speed, the half-step deviation arc difference complement algorithm also refers to the recursion method. According to the formula, it can be known that:

(1) When machining from the starting point of the arc, $F_0 = 0$, so use the formula:

$$\begin{aligned} f_0 &= 2F_0 + X_e - 2Y_e \\ &= X_e - 2Y_e \end{aligned} \tag{8}$$

Substituting the value of the actual interpolation arc target, the specific f_0 value is used to determine the feed direction, and its new deviation calculation is determined by the following methods.

(2) If $f_{ii} \geq 0$, the feed X direction is required, and the comparison deviation value of the next point is:

$$\begin{aligned} f_{i+1,i} &= 2F_{i+1,i} + X_e - 2Y_e \\ &= 2\left(F_{ii} - Y_e\right) + X_e - 2Y_e \\ &= F_{ii} + 2X_e - 2Y_e \\ &= f_{ii} - 2Y_e \end{aligned} \tag{9}$$

If $f_{ii} < 0$, $\triangle x$ and $\triangle y$ are fed, then the next deviation is:

$$\begin{aligned} f_{i+1,i+1} &= 2F_{i+1,i+1} + X_e - 2Y_e \\ &= 2\left(F_{ii} + X_e - Y_e\right) + X_e - 2Y_e \\ &= f_{ii} + 2X_e - 2Y_e \end{aligned} \tag{10}$$

According to the above derivation process, a similar formula can be derived when $X_e < Y_e$ or the end point coordinates are in other regions. This directly uses the deviation of the previous step to calculate, which simplifies the calculation formula and improves the calculation efficiency.

4. The Advantages of Half-step Deviation Method

4.1 Circular Interpolation Based on Half-step Deviation Method

A circle with a radius of 10 is processed separately below, and the interpolation results are shown in Figures 7 and 8 below.

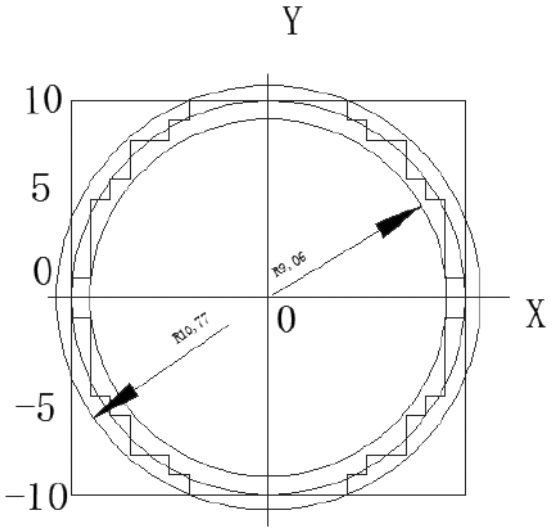

Figure 7. Circular Interpolation Based on Point-by-Point Comparison Method

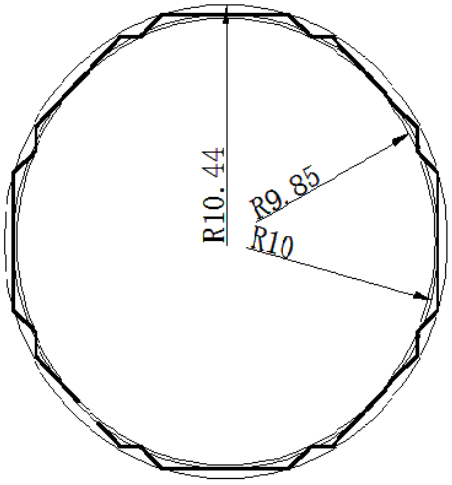

Figure 8. Circular Interpolation Based on Half-step Deviation Method

The interpolation principle of the point-by-point comparison method arc in Figure 7 is as follows: in the first quadrant, starting from the starting point of the arc, counterclockwise interpolation, when the discriminant is less than or equal to 0, go $+Y$, if it is bigger than 0, go to $-X$, and the other three quadrants and so on. and the entire in-

 DOI: https://doi.org/10.26549/met.v3i1.1603

terpolation route of Fig. 7 can be obtained.

The principle of circular interpolation of the half-step deviation method in Figure 8 is as follows: in the first quadrant, the starting point of the arc starts and counterclockwise interpolation. Before each interpolation, it is necessary to calculate which of the next two target points is closer to the arc (the distance from the arc is the smallest). After that, the corresponding pulse is sent, and then according to the region where the current point is located, the corresponding interpolation point is selected [in the first region is (-*X*, (-*X,* -*Y*)], for comparison, by analogy, the second region is selected [-*Y*, (+*X,* -*Y*)], and the entire interpolation route of Fig. 8 can be obtained according to the inverse circular interpolation shown in Figure 6.

The derivation process has been elaborated above, and the following conclusions can be seen as follows:

(1) After the interpolation by the half-step deviation method, the small circle R9.85 and the large circle R10.44, that is, the deviation contour at the time of interpolation, and the small circle by point-by-point comparison are R9.06 and the large circle R10.77. It is obvious that the accuracy of the half-step deviation method interpolation is high, and the error is within 0.5. According to the discriminating method given above, the interpolation path of the full circle can be derived.

(2) In the point-by-point interpolation comparison method in Figure 8, the whole circle with a processing radius of 10 needs to be calculated 80 times; while the half-step deviation method only needs to calculate 64 times to complete a full circle interpolation, which increases the efficiency by 20%.[8]

5. Conclusion

The point-by-point comparison method and the half-step deviation method are compared with the basic principle, the feed calculation rule, the feed discriminant, etc. The optimized half-step deviation method does not exceed 0.5 pulse equivalents in the interpolation arc error, which is reduced by half compared with the point-by-point comparison method. The half-step deviation method is less than the point-by-point comparison method, and the occupied storage space is small, and the multi-axis linkage and the number of interpolation steps can be reduced.

References

[1] Xiaochun Shu, Xiaoling Huang, Runhong Zhu. An Optimization Algorithm for Linear Interpolation Based on Point-by-Point Comparison Method[J]. Journal of Jining University, 2018, 39(05): 4-8. (in Chinese)

[2] Xiaochun Shu, Xiaoling Huang. Analysis of the Continuous Interpolation Algorithm for Small Line Segments in Numerical Control Machine Tools[J]. Management & Technology of SME (Early Issue), 2017(01):139-140. (in Chinese)

[3] Xiaochun Shu. Design and Implementation of Control and Fault Diagnosis System for Numerical Control Machine Tools[J]. Management & Technology of SME (Early Issue),2015(05):251-252. (in Chinese)

[4] Jinwen Li, Sumei He, Haibin Wu. A Linear Interpolation Algorithm and Its Application in Robots[J]. Journal of Mechanical & Electrical Engineering, 2015, 32(07):966-970. (in Chinese)

[5] Shujie Sun, Hu Lin, Liumo Zheng. Forward Interpolation Algorithm of NURBS Curve with Reverse Interpolation[J]. Journal of Computer-Aided Design & Computer Graphics, 2014, 26(09):1543-1549. (in Chinese)

[6] Jinglin Liu, Shuaifu Wang. The Control of Multi-step Motor Servo System for Numerical Control Machine Tools[J]. Electric Machines and Control, 2013, 17(05): 80-86. (in Chinese)

[7] Ying He. Analysis and Evaluation of Dynamic Behavior of High-speed Processing Interpolation Algorithm[D]. Huazhong University of Science and Technology,2005. (in Chinese)

[8] Chunlei Li, Gaolian Shi, Zhengwei Dai. Teaching Research and Design of Numerical Control Vehicle Circular Interpolation Instruction[J]. Guangxi Journal of Light Industry, 2018(4):152-153. (in Chinese)

DOI: https://doi.org/10.26549/met.v3i1.1603

About the Publisher

Synergy Publishing Pte. Ltd. (SP) is an international publisher of online, open access and scholarly peer-reviewed journals covering a wide range of academic disciplines including science, technology, medicine, engineering,education and social science. Reflecting the latest research from a broad sweep of subjects, our content is accessible worldwide – both in print and online.

SP aims to provide an analytics as well as platform for information exchange and discussion that help organizations and professionals in advancing society for the betterment of mankind. SP hopes to be indexed by well-known databases in order to expand its reach to the science community, and eventually grow to be a reputable publisher recognized by scholars and researchers around the world.

SP adopts the Open Journal Systems, see on *http://ojs.s-p.sg/*

About the Open Journal Systems

Open Journal Systems (OJS) is sponsored by the Public Knowledge Project Organization from Columbia University in Canada, jointly developed by PKP, the Canadian Academic Publishing Center and Canada Simon Fraser University Library. OJS can realize the office automation of periodical editing process, station build and full-text journals by network publishing. The system design is in line with international standards, and supports peer review. It is very helpful to improve the citation rate, academic level and publication quality of periodicals.

SYNERGY
PUBLISHING PTE. LTD.

ISSN 2591-7110
01
9 772591 711191

Synergy Publishing Pte. Ltd.
contact@s-p.sg
www.s-p.sg
12 Eu Tong Sen Street
#08-169 Singapore(059819)

MODERN ELECTRONIC TECHNOLOGY
is an independent open access journal published
by Synergy Publishing Pte. Ltd.